Published in final edited form as:

Cell. 2018 January 11; 172(1-2): 191–204.e10. doi:10.1016/j.cell.2017.11.003.

Rapid mobilization reveals a highly engraftable hematopoietic stem cell

Jonathan Hoggatt[1,2,3,10,*], **Pratibha Singh**[4], **Tiffany A. Tate**[2,3], **Bin-Kuan Chou**[1,2], **Shruti R. Datari**[1,2], **Seiji Fukuda**[5], **Liqiong Liu**[4], **Peter V. Kharchenko**[2,6], **Amir Schajnovitz**[2,3,7], **Ninib Baryawno**[2,3,7], **Francois E. Mercier**[2,3,7], **Joseph Boyer**[8], **Jason Gardner**[9], **Dwight M. Morrow**[9], **David T. Scadden**[2,3,7,*], and **Louis M. Pelus**[4,11,*]

[1]Harvard Medical School; Cancer Center and Center for Transplantation Sciences, Massachusetts General Hospital, Boston, MA 02129

[2]Harvard Stem Cell Institute, Cambridge, Massachusetts, 02138

[3]Department of Stem Cell and Regenerative Biology, Harvard University, Cambridge, MA 02138

[4]Department of Microbiology and Immunology, Indiana University School of Medicine, Indianapolis, IN 46202

[5]Department of Microbiology and Immunology, Indiana University School of Medicine; Currently Department of Pediatrics, Shimane University School of Medicine, Izumo, Shimane, Japan

[6]Department of Biomedical Informatics, Harvard Medical School, Boston, MA 02115

[7]Center for Regenerative Medicine, Massachusetts General Hospital, Boston, MA 02114

[8]Department of Statistical Sciences, GlaxoSmithKline, Collegeville, PA 19426

[9]Magenta Therapeutics, Cambridge, MA 02139; formerly GlaxoSmithKline, Collegeville, PA 19426

SUMMARY

Hematopoietic stem cell transplantation is a potential curative therapy for malignant and nonmalignant diseases. Improving the efficiency of stem cell collection and the quality of the cells acquired can broaden the donor pool and improve patient outcomes. We developed a rapid stem cell mobilization regimen utilizing a unique CXCR2 agonist, GROβ, and the CXCR4 antagonist AMD3100. A single injection of both agents resulted in stem cell mobilization peaking within

*Corresponding authors.

[10]Lead Contact: Jonathan Hoggatt, PhD, Cancer Center and Center for Transplantation Sciences, Massachusetts General Hospital. Formerly Stem Cell and Regenerative Biology, Harvard University – Scadden Lab. 149 13th Street, CNY 149 Room 5301, Boston, MA 02129. Phone: 617-726-6516; hoggatt.jonathan@mgh.harvard.edu Twitter: @jghoggatt

David T. Scadden, MD, Harvard Stem Cell Institute, Center for Regenerative Medicine, Massachusetts General Hospital, Department of Stem Cell and Regenerative Biology, Harvard University, 7 Divinity Avenue, Cambridge, MA 02138. Phone: 617-726-5615; david_scadden@harvard.edu

[11]Senior Author: Louis M. Pelus, Ph.D., Department of Microbiology and Immunology, Indiana University School of Medicine, 950 West Walnut Street, Indianapolis, IN 46202 Phone: 317-274-7565; Fax: 317-274-7592; lpelus@iupui.edu

AUTHOR CONTRIBUTIONS

Conceptualization, J.H. and L.M.P.; Methodology, J.H., S.F., A.S., N.B., F.M., L.M.P.; Validation, J.H., D.M.M., L.M.P.; Formal Analysis, P.V.K., J.B.; Investigation, J.H., P.S., T.A.T., B.K.C, S.D., A.S., N.B., F.M., L.M.P.; Resources, J.G.; Writing – Original Draft, J.H. and L.M.P.; Writing – Review and Editing, all authors; Supervision, J.H., D.T.S., L.M.P.; Funding Acquisition, J.H., D.T.S., L.M.P.

fifteen minutes that was equivalent in magnitude to a standard multi-day regimen of G-CSF. Mechanistic studies determined that rapid mobilization results from synergistic signaling on neutrophils, resulting in enhanced MMP-9 release, and unexpectedly revealed genetic polymorphisms in MMP-9 that alter activity. This mobilization regimen results in preferential trafficking of stem cells that demonstrate a higher engraftment efficiency than those mobilized by G-CSF. Our studies suggest a potential new strategy for the rapid collection of an improved hematopoietic graft.

Graphical abstract

A new strategy for stem cell mobilization enables rapid collection of an improved hematopoietic graft in humans

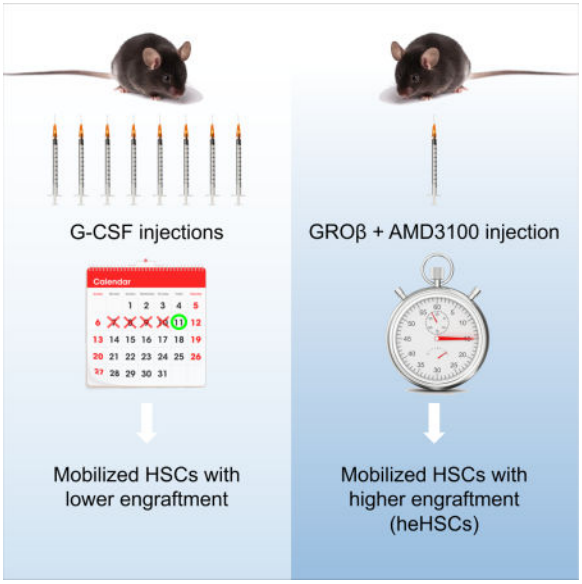

INTRODUCTION

Hematopoietic stem cell (HSC) transplantation has been used to treat malignant hematologic diseases for over 50 years. During this time, its therapeutic potential has expanded to non-malignant hematologic and immunologic disorders. With the emergence of gene therapy strategies and reduced toxicity conditioning regimens, hematopoietic transplantation is poised to expand to additional patient populations.

Successful transplantation requires harvesting of HSCs in both sufficient number and quality for robust engraftment, blood cell recovery, and lifelong maintenance of hematopoiesis. The predominant source of HSCs for transplant is mobilized peripheral blood (D'Souza et al., 2017; Niederwieser et al., 2016) that is acquired by apheresis of donor or patient blood after a multi-day regimen of granulocyte colony-stimulating factor (G-CSF). While successful, G-CSF regimens involve repeated injections and are often associated with bone pain, nausea, headache, and fatigue (Pulsipher et al., 2013; Pulsipher et al., 2009). The multi-day regimen and associated morbidities can be lifestyle disruptive and stressful for healthy volunteers

donating for allogeneic transplants and patients donating for autologous transplant. In a small population of healthy donors, G-CSF has been associated with serious toxicities, including splenic enlargement and rupture (Tigue et al., 2007). In high-risk individuals, the thrombophilic effects of G-CSF increase the risk of myocardial infarction and cerebral ischemia.

Despite its success for most patients and donors, poor mobilization rates as high as 40% have been reported (Giralt et al., 2014), and often those who do achieve sufficient numbers of hematopoietic stem and progenitor cells (HSPCs) require more than one apheresis procedure. Repeated, prolonged sessions of apheresis are particularly common amongst autologous donors and cause increased patient distress, tie up clinical resources, and increase the cost (Hosing et al., 2011; Shaughnessy et al., 2013).

Enhancing the standard of care for stem cell collection offers an opportunity to not only improve treatment of those who respond poorly to mobilization by G-CSF, but to expand autologous and allogeneic transplants across the full array of diseases that can potentially be cured.

RESULTS

GROβ is Well Tolerated in Humans and Modestly Increases Peripheral Blood CD34+ Cells

With the goal of developing a new mobilization regimen to overcome the shortcomings of the current standard of care, we began exploring an N-terminal 4-amino acid truncated form of the human chemokine GROβ. This molecule specifically binds to the CXCR2 receptor and with greater potency than full length GROβ (King et al., 2000). This truncated form is used throughout this manuscript and is simply referred to as GROβ. We previously showed that GROβ rapidly mobilizes HSPCs in mice (King et al., 2001; Pelus et al., 2004) and rhesus macaques (King et al., 2001).

Based on these animal studies, we performed a single-blind, dose escalating pilot study in humans to assess the tolerability and preliminary pharmacokinetics and pharmacodynamics following intravenous (iv) administration of GROβ in healthy volunteers. All subjects received matched placebo in the first session and a dose of GROβ in the second session, separated by at least 4 weeks. GROβ had no adverse effects on clinical laboratory parameters, ECG, cardiac output, vital signs or lung function, and was not antigenic in the population studied. Infusion of GROβ at doses ≥90 μg/kg resulted in reported acute lumbar region mid-line back pain, with a maximum tolerated dose of 200 μg/kg. Back pain was reported in 11 subjects (29.7%) following infusion with GROβ compared to 2 subjects (5.3%) receiving placebo and generally resolved without stopping drug infusion within 10 min. No other serious adverse events were reported. In subjects receiving doses ≥60 μg/kg, a modest but significant increase in peripheral CD34+ cell counts, a phenotypic measure of HSPCs, was observed compared to matched placebos (Figure 1A). The maximal CD34+ cell count measured was achieved following administration of GROβ in all but one subject (Figure 1B).

Simultaneous Administration of GROβ and AMD3100 Increases Hematopoietic Mobilization

Although GROβ was well tolerated in humans, the magnitude of mobilization was not expected to be sufficient for clinical harvesting. We previously reported that administration of GROβ following a standard G-CSF regimen increases mobilization in mice. However, this strategy would still require multi-day administration of G-CSF and thus would not be expected to substantially alter standard of care. Single administration with rapid mobilization kinetics would be more ideal. The CXCR4 antagonist AMD3100 (Plerixafor) is approved for clinical mobilization and is used in combination with G-CSF, often when G-CSF has failed to mobilize sufficient numbers of CD34+ cells. Administration of AMD3100 as a standalone agent has been explored in some patient and donor populations (Devine et al., 2008; Pantin et al., 2017). However, the level of mobilization is below that of G-CSF.

With our experience in the healthy volunteer study, we returned to laboratory mouse models to explore the efficacy of a combinatorial strategy using GROβ and AMD3100. In mouse models, the peak mobilization produced by subcutaneous (sc) administration of AMD3100 was approximately one hour post-treatment (Broxmeyer et al., 2005) and GROβ peaked within 15 min (King et al., 2001). Therefore, we first administered AMD3100, waited for 45 min, and then administered GROβ, with blood analysis 15 min later (Figure 2A). We hypothesized that this dosing strategy would provide peak mobilization for both agents, giving us the maximal response. However, contrary to this hypothesis, we saw no increase in mobilization over GROβ alone. We then altered our strategy and administered both agents simultaneously. Using this simultaneous dosing regimen, peak mobilization was seen within 15 min (Figure 2B and (Hoggatt and Pelus, 2012)). While each agent given alone had less mobilization than a standard regimen of G-CSF (Figure 2C), the simultaneous combination of GROβ+AMD3100 resulted in significantly greater mobilization than seen with the standard multi-day G-CSF regimen (Figure 2C).

Release of MMP-9 Correlates with Rapid Mobilization

Given that peak mobilization following GROβ+AMD3100 occurred within 15 min, mimicking the kinetics of GROβ alone, we hypothesized that the mechanism driving this enhanced mobilization was an enhancement of the GROβ mechanism. We previously demonstrated that GROβ mobilization is mediated by matrix metalloproteinase-9 (MMP-9) (King et al., 2001; Pelus et al., 2004). As seen previously, GROβ increased peripheral blood MMP-9 as measured by zymography (Figure 3A) and in addition we now also show similar results measured by ELISA (Figures 3B–D). The combination of GROβ+AMD3100 substantially increased MMP-9 levels (Figures 3A–D), compared to either agent used alone. Changes in plasma levels of tissue inhibitor of metalloproteinases 1 (TIMP-1), an endogenous inhibitor of MMP-9, were not seen after administration of any agents (Figure 3C), nor were there significant changes in bone marrow levels (not shown). We next assessed peripheral MMP-9 over a 24-hour period post-administration. Peak MMP-9 levels were seen within 5–15 min after the combination regimen (Figure 3E) and rapidly returned to baseline within 12 hours. Importantly, the kinetics of peripheral MMP-9 release matched the kinetics of mobilization (Figure 3F). Analysis of numerous independent experiments encompassing 112 individual mice, representing a variety of mouse strains and genetic variants (described in later sections), demonstrated a strong correlation between progenitor

cells mobilized to peripheral blood and plasma MMP-9 levels following GROβ or combination treatment (Figure 3G). These results suggest that the mechanism of action of the combinatorial regimen may be like that of GROβ alone, and be dependent on MMP-9.

Neutrophil MMP-9 Enables Rapid Mobilization

Based on the rapid kinetics and the strong correlation of MMP-9 with hematopoietic mobilization, we hypothesized that GROβ and AMD3100 acted through their respective CXCR2 and CXCR4 receptors on neutrophils, resulting in enhanced MMP-9 release. This hypothesis is represented in Figure 4A. We based this hypothesis on; our earlier findings with GROβ as a single agent; the large amounts of MMP-9 stored in neutrophil granules making them the logical source; the role of these receptors in differentially regulating neutrophil trafficking (Eash et al., 2010); and importantly, the presence of high levels of CXCR2 receptor on neutrophils, while relatively absent on HSPCs (Supplementary Figure 1). To demonstrate the role of neutrophils in mobilization, we treated mice with an anti-Gr-1 antibody to deplete neutrophils (Supplementary Figure 2). Significant mobilization was seen with the combinatorial regimen compared to either agent alone in isotype treated mice (Figure 4B), whereas neutrophil depletion resulted in a complete absence of GROβ-mediated mobilization, and dramatically decreased mobilization from the combination regimen. In contrast, mobilization with AMD3100 was unaffected by neutrophil depletion.

To demonstrate the role of CXCR4 in the combined response, we used conditional CXCR4 knockout mice as we have previously described (Hoggatt et al., 2013). Conditional deletion of CXCR4 on its own resulted in mobilization (Figure 4C). GROβ administration resulted in significantly more mobilization than in wild type mice. In this case, the conditional deletion of CXCR4 replaces the effect of AMD3100, resulting in enhanced mobilization. However, AMD3100 did not mobilize in knockout mice, as expected given its known target. Similarly, there was no additional mobilization with the combination of GROβ+AMD3100 in knockout mice compared to GROβ alone. Likewise, CXCR2 gene deletion significantly reduced mobilization to GROβ (Figure 4D) and prevented any additional mobilization over AMD3100 alone when used in combination.

To confirm the role of MMP-9 we used two approaches. First, we mobilized MMP-9 knockout mice and compared them to wild type controls. Mice deficient in MMP-9 failed to mobilize in response to GROβ (Figure 4E). Mobilization to AMD3100 was unaffected, demonstrating that MMP-9 is not a primary mechanism of AMD3100 on its own. Importantly, there was no additional mobilization with the combination regimen, demonstrating the necessity of MMP-9 for the GROβ+AMD3100 regimen. To further verify, we used an antibody neutralization approach. Mice were given a neutralizing antibody for MMP-9 two hours prior to treatment, and mobilization was compared to isotype-treated controls. As was the case with MMP-9 knockout mice, there was no mobilization in response to GROβ (Figure 4F). Mobilization to AMD3100 as a single agent was unaffected and there was no additional mobilization with the combination regimen.

The totality of these studies using genetic knockout mice and antibody approaches confirm the model hypothesized (Figure 4A). The rapid mobilization elicited by GROβ+AMD3100 is the result of an agonist effect of GROβ on neutrophil CXCR2 coincident with antagonism

of CXCR4 by AMD3100, resulting in release of MMP-9 and subsequent hematopoietic mobilization.

Human Neutrophils Release MMP-9 in Response to GROβ+AMD3100

The mouse studies described in Figure 4 suggested a crosstalk between the CXCR2 and CXCR4 receptors in neutrophils. Signaling from the CXCR4 receptor appeared to dampen CXCR2-mediated mobilization. To further explore this crosstalk, we utilized freshly harvested human neutrophils and treated them *ex vivo* with GROβ and AMD3100. Human neutrophils were used in these studies with an eye towards clinical translation of the rapid mobilization regimen but also out of practicality to acquire sufficient numbers for signaling analysis. In preliminary studies however, mouse peripheral and marrow neutrophils demonstrated similar responses to GROβ and AMD3100 as human neutrophils (not shown).

Signaling downstream of both CXCR2 and CXCR4 receptors is known to cause intracellular calcium mobilization (Duda et al., 2011; Waugh and Wilson, 2008). Human neutrophils treated with GROβ or SDF-1, the ligand for CXCR4, had an increase in calcium mobilization (Figure 5A, left panel). However, when the CXCR4 inhibitor AMD3100 was added, the calcium mobilization response to SDF-1 was blocked (Figure 5A, right panel). In contrast, GROβ+AMD3100 resulted in increased calcium mobilization over GROβ alone, demonstrating enhanced G-protein signaling after the combination.

We then pre-treated human neutrophils with pertussis toxin, an inhibitor of $G_{\alpha i}$, or mastoparan, an activator of $G_{\alpha i}$ signaling. The CXCR4 receptor is capable of activating $G_{\alpha i,}$ and previously shown to be pertussis toxin sensitive (Juremalm et al., 2000). GROβ treatment of neutrophils increased the release of active MMP-9, as measured by zymography (Figure 5B) and closely matched the molar ratio of MMP-9 and its inhibitor TIMP-1, as measured by ELISA (Figure 5C). When neutrophils were pre-treated with pertussis toxin there was a significant increase in MMP-9 release after GROβ treatment (Figure 5B, C). In this case, the inhibition of G-protein signaling mimics the effect of AMD3100, i.e., blocking CXCR4 signaling enhances the GROβ-mediated release of MMP-9. Similarly, mastoparan, which activates $G_{\alpha i}$ signaling and thus mimics CXCR4 agonism, blocked the GROβ-mediated release of MMP-9 (Figures 5B, C). In contrast, cholera toxin, which is an activator of $G_{\alpha s}$ signaling, had no effect (Figure 5D, E), validating the role of $G_{\alpha i}$ signaling pathways in the response.

To further determine the potential regulators of the combination regimen, we pretreated human neutrophils with signaling pathway inhibitors prior to treatment with GROβ, AMD3100, or the combination. Inhibition of p38 MAPK signaling with SB203580 (Figure 5F), or JAK2 with AG490 (Figure 5G), had no effect on GROβ-mediated release of MMP-9, or the enhanced release in response to the combination treatment. Pre-treatment with PI3K inhibitors, Wortmannin or LY294002, resulted in an increase in GROβ-mediated release of MMP-9 (Figures 5H and 5I, respectively), to a similar degree as combination treatment. Similarly, blockade of MEK1 signaling by PD98059 partially mimicked the effect of AMD3100. Distinct from the effects of these inhibitors in mimicking AMD3100, the Src family kinase inhibitor PP2 blocked GROβ-mediated release of MMP-9 as well as the enhanced release from the combination regimen (Figure 5K). This result suggests that Src

family kinases are a key signaling pathway downstream of CXCR2 governing MMP-9 release.

Mouse Strains Differentially Mobilize to GROβ + AMD3100

The donor and patient pool for hematopoietic mobilization is diverse, and the clinical experience with G-CSF has shown broad ranges in the ability to mobilize between individual donors (Vasu et al., 2008). Prior reports in mice have also shown differences in the capacity to mobilize in response to G-CSF or cyclophosphamide (Roberts et al., 1997; Watters et al., 2003). We assessed mobilization in C57Bl/6, DBA/2, or their F1 hybrid (BDF1). Mobilization with GROβ or the combination treatment was significantly greater in DBA/2, compared to C57Bl/6 mice (Figure 6A), while mobilization with AMD3100 did not differ amongst the strains. This result suggested that the strain differences were predominantly due to a GROβ-related mechanism. Indeed, when we assessed blood plasma levels for MMP-9 activity, DBA/2 mice exhibited more activity after GROβ or combination treatment than did C57Bl/6 mice (Figure 6B).

To further explore this differential mobilization, and to account for other potential differences in the bone marrow niche or vasculature, we performed similar experiments in chimeric mice. Lethally irradiated BDF1 mice were transplanted with DBA/2, C57Bl/6, or BDF1 bone marrow. In these mice, the microenvironment was the same and only the hematopoietic system differed. As we showed previously, DBA/2 mice had greater mobilization to GROβ and the combination of GROβ+AMD3100 than C57Bl/6 mice (Figure 6C). Similarly, DBA/2 chimeric mice demonstrated greater mobilization than C57Bl/6 chimeras (Figure 6D). These results demonstrate that the strain differences in mobilization response to GROβ are due to differences in the hematopoietic system.

Mouse Strains Differ in MMP-9 Hemopexin-like Domain

There are numerous genetic differences amongst strains of mice that could account for the differing mobilization response. However, given that the differences in our experiments seemed to be GROβ-dependent, as mouse strains did not differ in mobilization to AMD3100, coupled with the increased MMP-9 activity in the DBA/2 mice (Figure 6B), and the clear constraint to the hematopoietic system (Figure 6D), we hypothesized that the difference in mobilization to the combination regimen was mediated by genetic variation in MMP-9. Evaluation of the genomic sequence of MMP-9 in DBA/2 and C57Bl/6 mice identified two, single nucleotide polymorphisms (SNPs) between the strains at positions 639 and 711 (Figure 6E). These SNPs result in leucine to proline and histidine to proline switches at those positions. These polymorphisms exist in the hemopexin-like domain of MMP-9, where the inhibitor TIMP-1 binds (Cha et al., 2002; Van den Steen et al., 2006).

Given the difference in gelatinolytic activity between DBA/2 and C57Bl/6 mice after GROβ or combination treatment (Figure 6B), and the greater mobilization in DBA/2 mice compared to C57Bl/6 (Figures 6A,C), we hypothesized that the SNPs we found in the hemopexin-like domain may alter the binding of TIMP-1 to MMP-9, and thus alter activity. To test this hypothesis, we loaded equal amounts of MMP-9 isolated from DBA/2 or C57Bl/6 mice onto sepharose beads with immobilized TIMP-1. After washing, MMP-9 was

eluted off the beads and levels determined by ELISA. The MMP-9 acquired from DBA/2 mice eluted off the TIMP-1 beads more readily than did the MMP-9 from C57Bl/6 mice (Figure 6F), suggesting that the binding of TIMP-1 to MMP-9 in DBA/2 mice is not as strong as C57Bl/6 MMP-9, consistent with the newly found SNPs in the hemopexin-like domain.

Based on these findings, we reasoned that the strain differences in mobilization to our new regimen could be attributed to this specific genetic difference. To test this hypothesis, we created retroviral vectors containing scrambled, C57Bl/6 MMP-9 or DBA/2 MMP-9 transgene, with a GFP reporter, and transduced bone marrow cells from MMP-9 knockout mice (Figure 6G). After transduction, HSPCs were sorted based upon GFP expression and transplanted into cohorts of lethally irradiated MMP-9 knockout mice. This experimental setup created chimeric mice in which all the hematopoietic cells would express a specific form of MMP-9, independent of any other strain differences. As we observed in other experiments, un-manipulated MMP-9 knockout mice did not mobilize after GROβ treatment and C57Bl/6 mice mobilized to a lesser degree than DBA/2 mice (Figure 6H). Transplant of MMP-9 knockout mice with hematopoietic cells transduced with the C57Bl/6 MMP-9 transgene restored mobilization to GROβ and the combination treatment (Figure 6I). Similarly, transplant with the DBA/2 MMP-9 transgene-transduced cells restored mobilization that was greater than the C57Bl/6 transgene chimeras. These results reveal that these two SNPs in the MMP-9 gene result in significant differences in biologic activity.

GROβ Increases Bone Marrow Vascular Permeability

The rapid and robust mobilization kinetics of GROβ+AMD3100 made us curious as to potential changes in the bone marrow niche. Mobilization with G-CSF is known to cause numerous changes within the bone marrow, including a characteristic flattening of osteolineage cells, reduction of adhesion and chemoattractant molecules, etc. (Hoggatt and Pelus, 2011; Tay et al., 2017). In contrast to overt changes in the microenvironment we (Hoggatt et al., 2013) and others have seen with G-CSF, we did not observe histologic differences in the bone marrow environment or significant changes in adhesion molecule expression 15 min following GROβ+AMD3100 treatment (not shown). Since we previously used intra-vital imaging to observe HSCs within the bone marrow in dynamic settings (Lo Celso et al., 2009) we applied this technique to assess the microenvironment during our mobilization treatment. In a pilot study, we treated mice with vehicle control or the GROβ +AMD3100 combination. Five minutes after treatment, we injected the mice with a rhodamine dextran dye with the intent to label the vasculature. Quite unexpectedly, the large molecular weight dye leaked out of the bone marrow vessels in the GROβ+AMD3100 treated mice (Figure 6J and Supplementary Videos 1 and 2). Based on this surprising finding, we imaged numerous other mice after treatment with vehicle, GROβ, AMD3100 and the combination treatment. We observed an increase in vascular permeability with the combination regimen and to a lesser degree GROβ or AMD3100 alone (Figure 6K). Importantly, when mice were pre-treated with an anti-MMP-9 antibody prior to GROβ +AMD3100 treatment (Figure 4F), the increase in vascular permeability was completely blocked (Figure 6K and Supplementary Videos 3–5). These data demonstrate that

combination regimen release of MMP-9 rapidly increases bone marrow vascular permeability.

GROβ+AMD3100 Mobilizes a Superior Hematopoietic Graft

We next evaluated and compared the hematopoietic grafts mobilized by GROβ+AMD3100 compared to a standard multi-day regimen of G-CSF. Lethally irradiated mice transplanted with peripheral blood mononuclear cells (PBMC) from mice treated with the combination regimen had a 4-day faster recovery of neutrophils (Figure 7A) and a 6-day faster recovery of platelets (Figure 7B) compared to mice transplanted with a G-CSF graft. In competitive repopulation assays, competing PBMC to freshly harvested bone marrow cells, the grafts mobilized with GROβ+AMD3100 were significantly more competitive than G-CSF (Figure 7C). At 6 months, we performed secondary transplantation assays to determine long-term repopulating capacity. Surprisingly, not only did the marrow from mice that received a GROβ+AMD3100 graft outcompete the G-CSF group, the chimerism increased compared to the primary graft, while the G-CSF graft remained the same (Figure 7D). These data clearly demonstrated that the GROβ+AMD3100 regimen mobilized a graft that led to robust short and long-term engraftment, and was more competitive than G-CSF grafts.

GROβ+AMD3100 Mobilizes a Highly Engraftable Hematopoietic Stem Cell (heHSC)

One explanation for the slight rise observed in the secondary transplantation assay is that the GROβ+AMD3100 graft contained more long-term repopulating stem cells than the G-CSF graft. However, since these grafts consisted of total PBMCs we could not definitely rule out accessory cell effects. We first evaluated the PBMC grafts by flow cytometry for HSPCs using a standard antibody panel, focusing on the lineage^{negative} Sca-1^{+} c-kit^{+} (LSK) population, or the more defined stem cell population CD150^{+} CD48^{-} lineage^{negative} Sca-1^{+} c-kit^{+} (SLAM LSK). Despite the clear increase in hematopoietic engraftment in both non-competitive and competitive transplants (Figures 7A–D), there were less phenotypically defined HSPCs in the GROβ+AMD3100 graft compared to G-CSF (Figures 7 E–G). These results indicated that perhaps the rapid regimen mobilized a distinct stem cell population from that of G-CSF. To test this hypothesis, we repeated competitive transplantations using highly purified, FACS-sorted SLAM LSK cells from the peripheral blood of the mobilized mice and competitively transplanted the exact same number from each donor source. In three separate experiments, SLAM LSK cells acquired from mice treated with GROβ +AMD3100 were twice as competitive as those from G-CSF-treated mice (Figure 7H). Intriguingly, if we truncate transplants that resulted in 10% or less chimerism, the G-CSF sourced cells demonstrated low engraftment in 5 out of 17 mice, while no mice were below that threshold in the GROβ+AMD3100 grafts. There is only a $(1/2)^5 = 0.03125$ chance that all 5 animals would come from the G-CSF group if both groups had the same probability of low engraftment, further demonstrating the enhanced engraftment capability of the combination regimen. Grafts from both sources resulted in multi-lineage reconstitution (Figure 7 I, J), with no apparent lineage bias between sources.

These results demonstrate that the combination regimen of GROβ+AMD3100 mobilizes a distinct, highly engraftable hematopoietic stem cell (heHSC) population with superior competitiveness compared to G-CSF-mobilized HSCs. As a preliminary, pilot

characterization of the heHSC population, we mobilized new cohorts of mice with G-CSF or GROβ+AMD3100, sorted SLAM LSK cells from the peripheral blood and from the marrow, and performed RNA sequencing. Sequence analysis indicated that the heHSCs had a distinct transcriptome compared to G-CSF mobilized HSCs, or those acquired from bone marrow. Intriguingly, in a gene set enrichment analysis, when we compared the genes upregulated in heHSCs compared to G-CSF mobilized HSCs, there was a significant enrichment for genes upregulated in fetal liver HSCs (Ivanova et al., 2002), compared to bone marrow HSCs (Figure 7K). This gene signature was unique to the heHSCs mobilized by GROβ+AMD3100 as it was not seen with freshly harvested bone marrow HSCs (not shown), and was distinct from G-CSF mobilized HSCs that were exposed *ex vivo* to GROβ+AMD3100 (Supplementary Figure 3). These results suggest that not only do heHSCs have a distinct biologic function, they also have a unique transcriptome which partly mirrors that of young, fetal liver HSCs.

DISCUSSION

Based on the current clinical standard for stem cell mobilization, we believe that the next generation strategy should be: 1) rapid – not five days or more of injections and resultant life disruption, but a single treatment with harvesting the same day; 2) more efficient – an ideal regimen would have predictable and robust mobilization that could reliably acquire all the cells needed in a single apheresis session; 3) less toxic – avoids the multiple injections and side effects associated with modern mobilization; and 4) produce a superior stem cell graft – that repopulates hematopoiesis quicker, reducing infections and/or bleeding complications and hospital stay.

The GROβ+AMD3100 regimen meets many of these goals. In mice, mobilization peaks within 15 min. Clinically, this regimen potentially could also be accomplished with a single injection, or two simultaneous injections. For the donor, this would be a superior experience compared to multi-day regimens currently in use. Nearly all PBSC donors experience bone pain, and most of them within 24 hours of the first injection of G-CSF (Pulsipher et al., 2013; Pulsipher et al., 2009). Overall, GROβ was well tolerated in our healthy volunteer study. It will be important to assess pain and toxicity with the combination treatment in future clinical studies, but the single injection, single day procedure is likely to have considerable advantages over G-CSF. Importantly, grafts obtained with our new regimen resulted in quicker hematopoietic recovery, greater donor chimerism, and mobilized HSCs with superior competitiveness compared to grafts obtained from G-CSF mobilized donors.

The number of transplants being performed is increasing, as are the potential diseases that can be treated. As toxicities associated with conditioning continue to be reduced, coupled with strategies to reduce graft versus host disease, a steady supply of HSCs, and hence donors, will be needed to expand transplant as a treatment option. One potential barrier is donor recruitment and attrition, with many potential donors ultimately declining to donate (Kaster et al., 2014; Switzer et al., 2013; Switzer et al., 1999). Some factors include fear of needles or pain, the inconvenience of the donation process, a lack of time or worried about missing work, and general doubts and worries. A single injection, single day collection with

GROβ+AMD3100 could potentially reduce some of these barriers and increase the donor pool.

The benefit of a single day procedure, particularly for healthy donors, has been recognized by others who have explored AMD3100 as a standalone agent (Devine et al., 2008; Schroeder et al., 2017). However, roughly a third of donors fail to mobilize enough after a single treatment, and adequate collection fails in many even after multiple apheresis sessions. Dose escalation and a change from sc to iv administration of AMD3100 does not overcome these shortcomings (Schroeder et al., 2017). Our results suggest that the addition of GROβ along with AMD3100 may be enough to boost the efficacy of rapid, single day mobilization and warrants further clinical exploration.

Mechanistic studies in mice and human neutrophils clearly indicate that GROβ mobilization is enhanced by blocking CXCR4 signaling. These studies suggest that other CXCR4 antagonists such as ALT-1188, POL5551, or BKT140, are likely to also enhance GROβ mobilization. Intriguingly, the mechanism of action of simultaneous administration of GROβ +AMD3100 appears to be fundamentally different than that of AMD3100 on its own. AMD3100 is believed to act by inhibiting CXCR4 directly on stem and progenitor cells. In contrast, we have shown that combined administration of GROβ along with AMD3100 causes mobilization by targeting CXCR4 on neutrophils. This new mechanism of action results in faster kinetics of mobilization than AMD3100 on its own. The kinetics will need to be further explored in clinical studies, but these animal models support the potential of same day drug administration and stem cell harvesting.

We also found that the differing mobilization between the DBA/2 and C57Bl/6 strains of mice is due to 2 SNPs in the hemopexin-like domain of MMP-9. These polymorphisms alter the activity of MMP-9, resulting in a more active variant in DBA/2 mice. Genetic polymorphisms in the hemopexin domain of MMP-9 have also been reported in humans, and have shown correlations with cancer risk (Cotignola et al., 2007; Kessenbrock et al., 2010), cardiovascular disease (Luizon et al., 2016; Tanner et al., 2011) or even personality (Suchankova et al., 2012). Our studies in mice suggest that genetic differences in MMP-9 can have strong biologic effects independent of total protein levels. These results argue for more functional assays when evaluating polymorphisms in humans, and suggest a potential biomarker of response to our new mobilizing regimen.

Coincident with the MMP-9 release and mobilization, we saw a rapid increase in bone marrow vascular permeability following GROβ+AMD3100, that was completely blocked with an anti-MMP-9 neutralizing antibody. This increase in vascular permeability may open the doorway for hematopoietic egress (Itkin et al., 2016) and partly explain the rapid mobilization in our studies. Excitingly, the rapid egress results in enrichment of heHSCs that have superior engrafting capability. Strongly engrafting stem cells is ideal for all patients, but may be particularly useful in clinical scenarios where stem cell competitiveness may be impaired, such as gene modified stem cell transplantation. Not only do these heHSCs have a distinct engraftment advantage, but they also have a unique transcriptome. Given the lack of the CXCR2 receptor on these HSCs, and the fact that the transcriptome is distinct from mobilized HSCs exposed *ex vivo* to GROβ+AMD3100, strongly suggests that heHSCs are

an inherently unique population. Intriguingly, this transcriptomic difference in heHSCs versus traditionally acquired HSCs shares similarities with those of fetal liver HSCs. These similarities should not be interpreted to suggest the presence of fetal liver HSCs in adult mouse bone marrow, but rather likely reflect shared properties, some of which contribute to the enhanced engraftment capabilities. Further exploration is required to delineate specific genetic components governing the high engraftment.

While the existence of heterogeneity within the HSC pool is increasingly being recognized, there are few tools that allow prospective isolation of stem cells with differing function, particularly in humans. Rapid mobilization with GROβ+AMD3100 now facilitates a biologic “panning” approach to stem cell discovery. The differential mobilization process of G-CSF versus GROβ+AMD3100 acts as a biologic sieve, allowing for the reliable collection of heHSCs with distinct transcriptomics and engraftment. This approach may be a valuable tool to explore stem cell function, heterogeneity, and engineering.

STAR METHODS

Contact for reagent and resource sharing

Further information and requests for resources and reagents should be directed to and will be fulfilled by Jonathan Hoggatt, Hoggatt.Jonathan@mgh.harvard.edu. GROβ was obtained from GSK under MTA. Homozygous MMP-9-deficient C57Bl/6 mice (Vu et al., 1998) were obtained from Dr. Zena Werb, UCSF, San Francisco, CA and CXCR4 conditional mice (Nie et al., 2004) from Dr. Yung-Ru Zou, Columbia University, NY, NY.

Experimental model and subject details

Animals—SPF BALB/c, C57Bl/6, DBA/2, $B_6D_2F_1$ (BDF) and ICR/CD1 male and female mice (6–8 weeks old) were purchased from Jackson Laboratories or Charles River Laboratories, housed in laminar flow micro isolators with continuous access to sterilized rodent chow and acidified water and acclimated for 2 weeks before use. Homozygous MMP-9-deficient C57Bl/6 mice (Vu et al., 1998) were obtained from Dr. Zena Werb and bred at Indiana University School of Medicine (IUSM). Maintenance of the MMP-9-null phenotype was monitored by zymography. CXCR2 knockout and control mice and were obtained from Jackson Labs. Conditional CXCR4 knockout mice (Nie et al., 2004) were obtained from Dr. Yung-Ru Zou, Columbia University, NY, NY, and bred at IUSM. B6.SJL-Ptprc (BoyJ) mice were purchased from Jackson Labs or bred in the IUSCC In Vivo Therapeutics Core facility. For animals bred in house, littermates of the same sex were randomized to experimental groups. The animal care and use committee of Indiana University School of Medicine and Harvard University approved all protocols involving animals at their respective institutions. Unless otherwise stated, in all experiments, each mouse was assayed individually.

Healthy Volunteers—The study protocol (SB-251,353/002) and amendments, the informed consent, and other information that required pre-approval were reviewed and approved by the Independent Ethics Committee (IEC) at SmithKline Beecham. Written, dated, informed consent was obtained from each subject prior to the performance of any

study-specific procedures. Data for each subject was recorded in an electronic case report form (CRF), using the SmithKline Beecham (SB) Phase I information management system (PIMS).

As this study was the first administration of GROβ in humans, the study was conducted in young healthy male volunteers. GROβ (SB-251353) was formulated as 25 mg/mL SB-251353, 20 mM sodium acetate, 150 mM sodium chloride, 0.02% (w/v) Polysorbate 80 at pH 4.0. Placebo was formulated as 20 mM sodium acetate, 150 mM sodium chloride, 0.02% (w/v) Polysorbate 80 at pH 4.0. Each subject had to satisfy the following inclusion criteria before entry into the study:

1. Male subjects aged between 18 and 45 years inclusive.
2. Subjects had to have good diameter forearm veins on both arms, so that cannulae could be inserted and used for leukapheresis if required.
3. Subjects had to have healthy skin on both forearms so that the skin prick testing could be performed on the volar surface.
4. Body weight within 25% of ideal weight for height, according to the 1983 Metropolitan Life Weight Charts.
5. No abnormality on clinical examination. A subject with a clinical abnormality was included only if the principal investigator considered that the abnormality would not introduce risk factors and would not interfere with the study procedures.
6. No abnormality on clinical chemistry or hematology examination at the pre-study medical. Subjects with laboratory parameters outside the reference range for this age group were only included if the principal investigator considered that such findings would not introduce additional risk factors, except for hemoglobin levels which had to be within the normal laboratory range.
7. A 48-hour Holter ECG and 12-lead ECG at the pre-study medical, which was normal.
8. A negative pre-study urine drug screen.
9. A negative pre-study Hepatitis B surface antigen result within 3 months of the start of the study.
10. A negative anti-GROβ antibody test and negative skin prick test at screening.

Exclusion Criteria: A subject was excluded from the study if any of the following criteria applied:

1. Had experienced any allergic reaction to an *Escherichia coli*-derived protein before this study.
2. Had a history of asthma and/or atopy requiring medical therapy.
3. Had active arthritis or inflammatory skin conditions including psoriasis or eczema in the last 6 months.

4. Had a history of inflammatory eye disorder within the last year.
5. Had a history of venous thrombosis (deep vein thrombosis), or atherosclerosis.
6. Had a strong family history of myelodysplasia or myeloid leukaemia (in parents, children or siblings).
7. Had received prescribed medication within 14 days prior to the first dosing day which, in the opinion of the principal/co-investigator, would interfere with the study procedures or compromise the study.
8. Had received over the counter (OTC) medicine within 48 hours before the first study day. Subjects who had taken OTC medication could still enter the study if, in the opinion of the principal/co-investigator, the medication received would not interfere with the study procedures or compromise the study. In particular, any iron containing-preparations and -multivitamins could not be taken. Aspirin and ibuprofen were not permitted due to their anticoagulant affects on platelets. Paracetamol was permitted.
9. Had abuse of alcohol defined as an average weekly intake of greater than 21 units or an average daily intake of greater than 3 units (1 unit is equivalent to half a pint of beer or 1 measure of spirits or 1 glass of wine).
10. Had a history or presence of gastro-intestinal, hepatic or renal disease or other condition known to interfere with the absorption, distribution, metabolism or excretion of drugs.
11. Had exposure to more than 3 new chemical entities within 12 months prior to the first dosing day.
12. Had participated in a trial with any drug within 84 days before the start of the study.
13. Had participated in a trial with a different new chemical entity within 112 days before the start of the study.
14. If participation in the study would result in the subject having donated more than 1500 mL blood in the previous 12 months.
15. Had donated blood within 8 weeks of beginning the study.

In addition, as the effect of GROβ had not been studied on sperm, subjects were advised not to attempt to father a child either during the study or for 3 months after the last dose of GROβ.

Method Details

Peripheral blood (PB) mobilization and preparation of cell suspensions—

Several different mobilization strategies were employed. All compounds were administered subcutaneously (sc) GROβ 2.5 mg/kg and AMD3100 5 mg/kg were administered as single doses or in combination and PB analyzed at the indicated times. G-CSF was administered at 62.5 ug/kg/day, *bid*, and *sc* and peripheral blood analyzed ~ 16 hours after the last G-CSF dose. Injections were scheduled so that control and mobilized mice were evaluated at the

same time in every experiment. Mice were sacrificed by CO_2 asphyxiation and blood was obtained by cardiac puncture using EDTA-coated syringes. Plasma was isolated from aliquots of blood for each animal and stored at −20°C. Peripheral blood mononuclear cells (PBMC) were obtained by separation on Lympholyte-Mammal® (Cedarlane Labs Ltd, Hornby, Ontario, Canada) as described (Hoggatt et al., 2014). Marrow cells were harvested by flushing femurs with 1.0 mL of ice-cold PBS. CBCs were performed on a Hemavet Mascot (CDC Technologies, Oxford, CT). Manual differentials were performed on Wrights-Giemsa stained (Hema-Tek 1000, Bayer Corp, Elkhardt, IN) blood smears or bone marrow cell (bmc) cytospin preparations (Shandon Inc., Pittsburgh, PA).

Isolation of mouse and human PMN—Peripheral blood was centrifuged at 500g and the cell pellet resuspended in 1 ml EDTA/HBSS/BSA buffer. One mL cell suspensions of blood or marrow cells were layered on gradients of 78%, 69% and 52% Percoll® (RediGrad™ Percoll, <2 U/ml Endotoxin, Amersham Biosciences, Piscataway, NJ) in HBSS, prepared from a stock solution 9 parts Percoll and 1 part 10X HBSS (100% Percoll) and centrifuged at 500g for 30 minutes at ambient temperature. The refractive index (RI) of each Percoll layer was measured in a refractometer and density (δ) of the layer calculated according to the manufacturer's directions (52% Percoll, RI 1.347, δ=1.083 g/ml; 69% Percoll, RI 1.349, δ=1.090 g/ml; 78% Percoll, RI 1.350, δ=1.110 g/ml). Mature neutrophils were recovered from the 69%/78% interface and were positive for Gr-1 and Mac-1 by flow cytometry. Contaminating erythrocytes were removed by hypotonic lysis. Purity of PMN was determined on Wrights-Giemsa stained cytospin preparations. Peripheral blood and bone marrow PMN purities of 95.6 ± 4.3 % and 93.8 ± 0.4 %, respectively, were routinely obtained. Human PMN were isolated from EDTA blood obtained from healthy volunteers after informed consent and IRB approval. Erythocytes were lysed with RBC lysis buffer and PMN isolated on 1-Step polymorph (Accurate Chemical and Scientific Corporation, Westbury, NY) according to the manufacturer's instructions. Cytospin analysis confirmed that the population consisted of polymorphonuclear cells (>95%).

Preparation of marrow extracellular extracts—Immediately following CO_2 asphyxiation and cardiac puncture, femurs were removed and the contents of 1 femur from each mouse flushed with 1.0 mL of ice cold PBS using a 1 cc syringe with a 26g needle. The marrow plug was dispersed by refluxing through the 26g needle, centrifuged at 4000 rpm for 4 min in a micro centrifuge and aliquots of cell free supernates frozen at −20°C.

In vivo depletion of PMN—In order to evaluate the contribution of PMN to stem cell mobilization, PMN were depleted by administration of 150 ug/mouse of the monoclonal anti-PMN antibody (anti-GR1, clone RB6-8C5) before mobilization. Anti-GR-1 was administered 24 hours before GROβ administration. In every experiment, control animals were subjected to the identical mobilization regimens and treated with 150 ug/mouse of rat anti-mouse IgG2b isotype control mAb (eBiosciences). Flow cytometry and manual CBC analysis validated neutrophil depletion (see Figure S2).

MMP-9 antibody neutralization in vivo—In GROβ mobilization studies, mice received an IV bolus of either isotype-matched control mAb or 3 mg/kg neutralizing anti-MMP-9

antibody 2 hours before receiving 2.5 mg/kg GROβ. Peripheral blood CFU-GM were quantitated 15 min after GROβ administration; vascular permeability was assessed 5 minutes after GROβ injection.

CFU-GM assay—PBMC and unseparated marrow cells were assayed for CFU-GM in McCoy's 5A media with 15% heat-inactivated fetal bovine serum (Hyclone Sterile Systems, Logan UT) and 0.3% agar (Difco Laboratories, Detroit, MI) (Pelus et al., 2004). CFU-GM content of blood was determined by plating a defined numbed of PBMC and calculating based on CBC values, or by plating a defined volume of RBC lysed blood, as we have described (Hoggatt et al., 2014). Colonies were manually counted in a blinded fashion.

Analysis of WBC Recovery—Mice were mobilized with G-CSF or GROβ and AMD3100 and 2×10^6 mobilized PBMC transplanted non-competitively into cohorts of 10 lethally irradiated recipients per group. A cohort of non-irradiated mice was bled on the same schedule as the experimental groups. Every other day, 5 mice from each group were bled and neutrophils and platelets enumerated using a Hemavet 950FS. Alternate groups of 5 mice were bled on each successive bleeding time point so that mice were only bled once every 4 days. Recovery of neutrophils and platelets to 50% and 100% were determined by comparison to the average neutrophil and platelet counts in the control group throughout the experimental period as we have previously described (Hoggatt et al., 2013).

Flow cytometry—Isolation of mobilized PBMC, lineage depletion and flow cytometric analysis and FACS sorting of mobilized SKL and SLAM-SKL cells was performed as previously described (Fukuda et al., 2015; Hoggatt et al., 2013). All flow cytometry analyses were performed on an LSRII flow cytometer (BD). Cell sorting was performed on BD FACSAria flow cytometers.

RNA Sequencing—For HSC analysis, 200 SLAM SKL cells were directly sorted into 5 uL TCL lysis buffer (Qiagen, #1031576) in duplicate experiments. Library preparation was performed by the Smart-Seq2 protocol with subsequent RNA sequencing by Illumina NextSeq500 at the Broad Institute, Cambridge, MA.

Competitive PBMC and BM transplantation—In competitive transplant studies, PBMC from mobilized C57Bl/6 (CD45.2) mice were transplanted at a 2:1 ratio with 5×10^5 congenic Boy/J whole bone marrow competitor cells (CD45.1) into lethally irradiated (1100 cGy TBI; 550 cGy split dose, 6 hrs apart) BoyJ recipient mice. Peripheral blood chimerism and multi-lineage reconstitution was assessed out to 6 months. After 24 weeks, 1×10^6 bone marrow cells from primary recipients were transplanted non-competitively into lethally irradiated Boy/J recipients and peripheral blood chimerism and multi-lineage reconstitution monitored for an additional six months.

For analysis of head-to-head stem cell repopulation ability, cohorts of 20 C57Bl/6 mice were mobilized with a standard 4 day regimen of G-CSF or single combined administration of GROβ + AMD3100, PBMC isolated, lineage depleted, sorted for SLAM-SKL cells, and equal numbers of G-CSF or GROβ + AMD3100 mobilized SLAM-SKL cells transplanted competitively with 250,000 WBM cells from BoyJ mice into lethally irradiated BoyJ mice.

Peripheral blood chimerism was monitored at 16, 24 and 36 weeks. Multi-lineage reconstitution was monitored at 24 weeks.

Chimeric mouse strain generation and mobilization—Chimeras were generated using DBA/2, B6D2F1 and C57Bl6 donor cells transplanted into BDF1 recipients. Age and sex matched B6D2F1 mice were lethally irradiated (1100 cGy, split dose) and transplanted with 1×10^6 WBM cells from either DBA/2, B6D2F1 or C57Bl6 mice. At 8 weeks post-transplant wild type and chimeric mice were mobilized by GROβ and AMD3100 alone or in combination as described earlier. All mice recovered from irradiation following transplant and no overt signs of GVHD were seen in these chimeras.

Gelatin Zymography—Gelatinolytic activity in plasma or cell supernates was measured by zymography as previously described (Pelus et al., 2004). MMP-9 and MMP-2 bands were confirmed by comparison with MW standards and recombinant enzymes (R&D Systems). Band intensities were quantitated by densitometry and compared to a standard curve of rmMMP-9. Band intensities on digitized gels were quantified in Adobe Photoshop (Adobe Systems, San Jose, CA).

Measurement of mouse SDF-1, pro-MMP-9, TIMP-1 and human TIMP-1 by ELISA—Mouse pro-MMP-9 was measured using the mouse pro-MMP-9 Quantikine® ELISA (R&D Systems) according to the manufacturer's instructions. Mouse and human TIMP-1 were measured by sandwich ELISA per manufacturer's instructions.

Mouse PMN MMP-9 binding to TIMP-1—Neutrophils were isolated from peripheral blood of C57Bl/6 or DBA/2 mice as described above, washed, suspended at a concentration of 2×10^6 cells/ml in PBS and lysed on ice using a Polytron homogenizer. Mouse proMMP-9 in lysates was determined by ELISA and equal amounts of proMMP-9 were bound to hTIMP1 covalently linked to Sepharose beads using the MMP Purification kit (IP970, R&D Systems). After washing, active MMPs were released by acidic elution and neutralized per the manufacturer's instructions. Eluted MMP-9 was subsequently determined by ELISA.

Intracellular Ca^{+2} mobilization—Freshly purified human PMN (2×10^6/ml) were washed with PBS and loaded with 2.5 uM FURA-2 AM (Molecular Probes, Eugene, OR) in Kreb's Ringer buffer supplemented with 1 mg/ml BSA, 1 mM $CaCl_2$ and 1 mM $MgCl_2$ at 37 °C for 35 min. Cells were washed twice incubated for 15 min at 37 °C, pelleted and suspended at a concentration of 2×10^6 in ice cold Kreb's Ringer with 1 mg/ml Gelatin, 1 mM $CaCl_2$ and 1 mM $MgCl_2$ and kept on ice. Cells were placed in a continuously stirred cuvette at 37°C in a MSIII fluorimeter (Photon Technology, South Brunswick, NJ). Fluorescence was monitored at 340 and 380 nm for excitation and 510 nm for emission. Experiments were performed on the fly. Baseline excitation was evaluated for 30 seconds, paused and then cells were stimulated with GROβ or rhSDF-1 and recording restarted. In some experiments, AMD3100 was added at the start of the experiment and additions added at ~45 seconds. All data were recorded on printed tracings of relative fluorescence.

In vitro mutagenesis and retrovirus transduction—*In vitro* mutagenesis on the mouse MMP-9 cDNA was performed as previously described (Fukuda et al., 2004). Full

length mouse MMP-9 cDNA that confers open reading frame was amplified by RT-PCR from total RNA harvested from bone marrow cells of C57BL/6 mice using random hexamers and primers 5′-CTC ACC ATG AGT CCC TGG CAG CCC CTG-3′ and 5′-TCA AGG GCA CTG CAG GAG GTC GTA-3′. The cDNA was cloned into the TOPO plasmid (Invitrogen, Carlsbad, CA) and used for *in vitro* mutagenesis. The primers to substitute Leucine at position 639 with Proline (L639P) were 5′-phospho-CGG GAA GGC TCT GCT GTT CAG-3′ and 5′-phospho-GGA CGA CGC GGG AGA AGC CCG-3′. Primers to alter Histidine at position 711 to Proline (H711P) were 5′-phospho-TGA GGT GAA CCA GGT GGA CGA-3′ and 5′-phospho-GGG TCC ACC TTG TTC ACC TCA-3′. PCR was carried out for 30 cycles using phosphorylated primers to introduce L639P, and the MMP-9 cDNA in the TOPO plasmid as a template. The resultant product was digested with *Dpn*I followed by self-ligation and transformation into E.coli. Several clones were sequenced and the presence of L639P was verified. Subsequently, additional PCR was carried out to introduce H711P using MMP9-cDNA containing L639P in a similar manner. The cDNA harboring both L639P and H711P was cloned into the IRES-EGFP bicistronic plasmid MIEG3 vector by using *Eco*RI adaptor. Retrovirus transduction of MMP-9 constructs (wild type and mutant) into primary mouse bone marrow cells was performed as previously described (Fukuda et al., 2015; Fukuda et al., 2004; Fukuda et al., 2009).

Intravital microscopy—Live imaging of the mouse calvarial bone marrow was performed using a custom-built hybrid confocal and multi-photon microscope incorporating a fiber-based femtosecond laser (Cazadero FLCPA, Calmar laser) whose output at 1550 nm was extended to 1900 nm by soliton self frequency shifting though a photonic crystal fiber. The 1550 and the 1900 nm beams are doubled to 775 and 950 nm for simultaneous two-photon excitation. A water-immersion 60×/1.00w objective (LUMPLFLN60XW, Olympus) provided a 415×415 μm field of view, and Z-stacks were acquired to a depth of 150–200 μm at 1–5 μm Z-steps. Mice were maintained under anesthesia (1.35% isoflurane/oxygen mixture) and body core temperature was maintained. A U-shaped incision on the scalp exposed the calvarium bone, to which 2% methylcellulose gel was applied for refractive index matching. Second harmonic generation signal (SHG, excited at 775 nm) was used to visualize bone collagen and to locate calvarial bone marrow cavities for vasculature permeability measurements. Then, on-stage retro-orbital injection of 70 KDa rhodamine-dextran conjugate (150 μL of 3.3 mg/mL D-1841, Life Technologies) was performed. Bone collagen signal (SHG) and rhodamine-dextran signal (excited at 585 nm) were continuously recorded (13 frames/second) for 2 minutes after injection. For the quantification of Rhodamine-dextran leakage to the marrow space, videos were analyzed using ImageJ (NIH) to measure the increased fluorescent signal in 5 distinct regions of interest outside of blood vessels (figures depicting average of 5 ROIs per video).

Statistical analysis

Statistical analysis was made using the Prism software (Prism, GraphPad Software Inc., San Diego, CA USA), unless otherwise indicated. Differences between multiple means were evaluated by ANOVA with Tukey-Kramer multiple comparison test. In some cases, differences between means were evaluated using the unpaired 2-tailed *t* test function. The nonparametric Spearman correlation analysis (Figure 3G) was used for comparison of

MMP-9/TIMP-1 ratio and mobilized CFU-GM, and significance was defined as two-tailed $p < 0.001$.

For neutrophil and platelet recovery assays (Figures 7A,B) confidence intervals for the difference in time to 50% recovery between groups were obtained using bootstrap simulations. These simulations took mean recovery times from smoothing splines fit to the data for each group, and assessed the variability of these recovery times by using a mean-variance relationship estimated from the data. This mean-variance relationship was itself a smoothing spline relating standard deviations to means at observed time points.

For healthy volunteer CD34+ cell levels (Figure 1A), we formally estimated and tested for the effect of the drug on AUC in a statistical model that allowed for random effects across subjects and allowed for the effect of drug to differ between high (>=60 ug/kg) as opposed to low concentrations. Although we did not expect an effect of the drug at times later than 4 hours, we used the data past the four-hour timepoint to give a better estimate of the underlying variability. Specifically, we split the data into three periods – early (0–4 hours), middle (4–12 hours), and late (12–24 hours). We calculated log2(AUC) for each subject in each time period for each treatment regimen, and normalized each value by subtracting by the average log2(AUC) over all subjects and regimens for the same time period. Then we estimated the following model using the lmer function from the lme4 package in R (version 3.3.1):

$$\begin{aligned}\mathrm{NormLog2AUC} = {} & \mathrm{Drug} + \mathrm{TimePeriod} + \mathrm{HighConc} + \mathrm{Drug{:}TimePeriod} \\ & + \mathrm{Drug{:}HighConc} \\ & + \mathrm{TimePeriod} + \mathrm{HighConc} + \mathrm{Drug{:}TimePeriod} + \mathrm{HighConc},\end{aligned}$$

where Drug = 1 for drug, 0 for placebo; HighConc = 1 if in the high concentration group, 0 if otherwise; TimePeriod = Early, Middle, Late (categorical variable). Also, we allowed for a subject random effect. We used the model built in R to conduct a likelihood ratio test for the effect of Drug using the anova function in base R to compare it to the model without any terms involving Drug. The p-value was 0.001.

For the sorted stem cell transplantation assays we estimated the following statistical model using data for weeks 16, 24, and 36:

$$\mathrm{Log}_{10}(\mathrm{Pct\_\ Chimerism}_{\mathrm{i}}) = \beta_0 + \beta_1 * \mathrm{Therapy}_{\mathrm{i}} + \varepsilon_{\mathrm{ai}} + \varepsilon_{\mathrm{ei}} + \varepsilon_{\mathrm{ewi}} + \varepsilon_{\mathrm{ewti}} + \varepsilon_{\mathrm{i}},$$

where β_1 captures the effect of Therapy (GROβ + AMD3100 combination or G-CSF), ε_a is a normally-distributed mean zero animal random effect (one value for each animal, with standard deviation σ_a), ε_e is a normally-distributed mean zero experiment random effect (one value for each experiment), ε_{ew} is a normally-distributed mean zero experiment-week random effect (one value for each experiment and week, allowing for differences across weeks within an experiment), ε_{ewt} is a normally-distributed mean zero experiment-week-therapy random effect, capturing deviations in the effect of the therapies across weeks within

an experiment, and ε is a normally-distributed mean zero random effect with standard deviation σ, capturing variability for individual measurements.

In order to reduce the influence of outliers on the result, we re-estimated the model after truncating the low value of Pct_Chimerism at 10% and reducing the value of the large positive outlier for the GROβ + AMD3100 group in the 50-cell experiment in week 16 to 65. Both of these adjustments favor the finding no difference against the treatments, so that p-values calculated from the resulting data are conservative.

We estimated the model with the lmer function in the lme4 package in R (version 3.1.1). From this output we took our estimates of β_1 and the standard deviations of the variance components, and we obtained the lower confidence bound for β_1 using the confint.merMod function. We obtained the p-value for the test of $\beta_1=0$ using the anova function in the lmerTest package. Finally, it's worth pointing out that we have used one-sided rather than two-sided tests and confidence bounds in considering the null hypothesis the two therapies are equally good. This is justified by the fact that the alternative hypothesis going into the study was that the GROβ + AMD3100 combination would be better.

Supplementary Material

Refer to Web version on PubMed Central for supplementary material.

Acknowledgments

We are grateful to Dr. Charles P. Lin for development of the in vivo imaging system, and Dr. Zena Werb and Dr. Dr. Yung-Ru Zou for providing genetic mice. This work was supported by NIH Grant R00 HL119559 to J.H., NIH Grants HL069669 and HL096305 to L.M.P., the Massachusetts Life Sciences Center to D.T.S., R01HL131768 to P.V.K., and sponsored research from GlaxoSmithKline to L.M.P. and D.T.S. Flow cytometry and mice were partially funded by NCI grant P30 CA082709, NIDDK grant U54 DK106846, NIH instrumentation grant 1S10D012270, and NIAMS grant R01AR060332. J.H., D.T.S. and L.M.P. have filed patent applications. L.M.P was an employee of GSK (SmithKline Beecham) when he discovered and cloned the truncated GROβ molecule. J.G., D.M.M. and J.B. were employees of GSK at the time of this work. J.G. and D.M.M. are employees of Magenta Therapeutics. J.H., J.G., D.M.M. and D.T.S. are shareholders for Magenta Therapeutics.

References

Broxmeyer HE, Orschell CM, Clapp DW, Hangoc G, Cooper S, Plett PA, Liles WC, Li X, Graham-Evans B, Campbell TB, et al. Rapid mobilization of murine and human hematopoietic stem and progenitor cells with AMD3100, a CXCR4 antagonist. J Exp Med. 2005; 201:1307–1318. [PubMed: 15837815]

Cha H, Kopetzki E, Huber R, Lanzendorfer M, Brandstetter H. Structural basis of the adaptive molecular recognition by MMP9. J Mol Biol. 2002; 320:1065–1079. [PubMed: 12126625]

Cotignola J, Reva B, Mitra N, Ishill N, Chuai S, Patel A, Shah S, Vanderbeek G, Coit D, Busam K, et al. Matrix Metalloproteinase-9 (MMP-9) polymorphisms in patients with cutaneous malignant melanoma. BMC Med Genet. 2007; 8:10. [PubMed: 17346338]

D'Souza A, Lee S, Zhu X, Pasquini M. Current Use and Trends in Hematopoietic Cell Transplantation in the United States. Biol Blood Marrow Transplant. 2017

Devine SM, Vij R, Rettig M, Todt L, McGlauchlen K, Fisher N, Devine H, Link DC, Calandra G, Bridger G, et al. Rapid mobilization of functional donor hematopoietic cells without G-CSF using AMD3100, an antagonist of the CXCR4/SDF-1 interaction. Blood. 2008; 112:990–998. [PubMed: 18426988]

Duda DG, Kozin SV, Kirkpatrick ND, Xu L, Fukumura D, Jain RK. CXCL12 (SDF1alpha)-CXCR4/CXCR7 pathway inhibition: an emerging sensitizer for anticancer therapies? Clin Cancer Res. 2011; 17:2074–2080. [PubMed: 21349998]

Eash KJ, Greenbaum AM, Gopalan PK, Link DC. CXCR2 and CXCR4 antagonistically regulate neutrophil trafficking from murine bone marrow. The Journal of clinical investigation. 2010; 120:2423–2431. [PubMed: 20516641]

Fukuda S, Hoggatt J, Singh P, Abe M, Speth JM, Hu P, Conway EM, Nucifora G, Yamaguchi S, Pelus LM. Survivin modulates genes with divergent molecular functions and regulates proliferation of hematopoietic stem cells through Evi-1. Leukemia. 2015; 29:433–440. [PubMed: 24903482]

Fukuda S, Mantel CR, Pelus LM. Survivin regulates hematopoietic progenitor cell proliferation through p21WAF1/Cip1-dependent and -independent pathways. Blood. 2004; 103:120–127. [PubMed: 12969960]

Fukuda S, Singh P, Moh A, Abe M, Conway EM, Boswell HS, Yamaguchi S, Fu XY, Pelus LM. Survivin mediates aberrant hematopoietic progenitor cell proliferation and acute leukemia in mice induced by internal tandem duplication of Flt3. Blood. 2009; 114:394–403. [PubMed: 19411632]

Giralt S, Costa L, Schriber J, Dipersio J, Maziarz R, McCarty J, Shaughnessy P, Snyder E, Bensinger W, Copelan E, et al. Optimizing autologous stem cell mobilization strategies to improve patient outcomes: consensus guidelines and recommendations. Biol Blood Marrow Transplant. 2014; 20:295–308. [PubMed: 24141007]

Hoggatt J, Mohammad KS, Singh P, Hoggatt AF, Chitteti BR, Speth JM, Hu P, Poteat BA, Stilger KN, Ferraro F, et al. Differential stem- and progenitor-cell trafficking by prostaglandin E2. Nature. 2013; 495:365–369. [PubMed: 23485965]

Hoggatt J, Pelus LM. Many mechanisms mediating mobilization: an alliterative review. Curr Opin Hematol. 2011; 18:231–238. [PubMed: 21537168]

Hoggatt J, Pelus LM. Hematopoietic stem cell mobilization with agents other than G-CSF. Methods in molecular biology (Clifton, NJ). 2012; 904:49–67.

Hoggatt J, Tate TA, Pelus LM. Hematopoietic stem and progenitor cell mobilization in mice. Methods in molecular biology (Clifton, NJ). 2014; 1185:43–64.

Hosing C, Smith V, Rhodes B, Walters K, Thompson R, Qazilbash M, Khouri I, de Lima M, Balzer RJ, McMannis J, et al. Assessing the charges associated with hematopoietic stem cell mobilization and remobilization in patients with lymphoma and multiple myeloma undergoing autologous hematopoietic peripheral blood stem cell transplantation. Transfusion. 2011; 51:1300–1313. [PubMed: 21575005]

Itkin T, Gur-Cohen S, Spencer JA, Schajnovitz A, Ramasamy SK, Kusumbe AP, Ledergor G, Jung Y, Milo I, Poulos MG, et al. Distinct bone marrow blood vessels differentially regulate haematopoiesis. Nature. 2016; 532:323–328. [PubMed: 27074509]

Ivanova NB, Dimos JT, Schaniel C, Hackney JA, Moore KA, Lemischka IR. A stem cell molecular signature. Science. 2002; 298:601–604. [PubMed: 12228721]

Juremalm M, Hjertson M, Olsson N, Harvima I, Nilsson K, Nilsson G. The chemokine receptor CXCR4 is expressed within the mast cell lineage and its ligand stromal cell-derived factor-1alpha acts as a mast cell chemotaxin. Eur J Immunol. 2000; 30:3614–3622. [PubMed: 11169404]

Kaster EC, Rogers CR, Jeon KC, Rosen B. Getting to the Heart of Being the Match: A Qualitative Analysis of Bone Marrow Donor Recruitment and Retention Among College Students. Health Educ (Muncie). 2014; 46:14–19. [PubMed: 25632376]

Kessenbrock K, Plaks V, Werb Z. Matrix metalloproteinases: regulators of the tumor microenvironment. Cell. 2010; 141:52–67. [PubMed: 20371345]

King AG, Horowitz D, Dillon SB, Levin R, Farese AM, MacVittie TJ, Pelus LM. Rapid mobilization of murine hematopoietic stem cells with enhanced engraftment properties and evaluation of hematopoietic progenitor cell mobilization in rhesus monkeys by a single injection of SB-251353, a specific truncated form of the human CXC chemokine GRObeta. Blood. 2001; 97:1534–1542. [PubMed: 11238087]

King AG, Johanson K, Frey CL, DeMarsh PL, White JR, McDevitt P, McNulty D, Balcarek J, Jonak ZL, Bhatnagar PK, et al. Identification of unique truncated KC/GRO beta chemokines with potent

hematopoietic and anti-infective activities. J Immunol. 2000; 164:3774–3782. [PubMed: 10725737]

Lo Celso C, Fleming HE, Wu JW, Zhao CX, Miake-Lye S, Fujisaki J, Cote D, Rowe DW, Lin CP, Scadden DT. Live-animal tracking of individual haematopoietic stem/progenitor cells in their niche. Nature. 2009; 457:92–96. [PubMed: 19052546]

Luizon MR, Belo VA, Fernandes KS, Andrade VL, Tanus-Santos JE, Sandrim VC. Plasma matrix metalloproteinase-9 levels, MMP-9 gene haplotypes, and cardiovascular risk in obese subjects. Mol Biol Rep. 2016; 43:463–471. [PubMed: 27146834]

Nie Y, Waite J, Brewer F, Sunshine MJ, Littman DR, Zou YR. The role of CXCR4 in maintaining peripheral B cell compartments and humoral immunity. J Exp Med. 2004; 200:1145–1156. [PubMed: 15520246]

Niederwieser D, Baldomero H, Szer J, Gratwohl M, Aljurf M, Atsuta Y, Bouzas LF, Confer D, Greinix H, Horowitz M, et al. Hematopoietic stem cell transplantation activity worldwide in 2012 and a SWOT analysis of the Worldwide Network for Blood and Marrow Transplantation Group including the global survey. Bone Marrow Transplant. 2016; 51:778–785. [PubMed: 26901703]

Pantin J, Purev E, Tian X, Cook L, Donohue-Jerussi T, Cho E, Reger R, Hsieh M, Khuu H, Calandra G, et al. Effect of high-dose plerixafor on CD34+ cell mobilization in healthy stem cell donors: results of a randomized crossover trial. Haematologica. 2017; 102:600–609. [PubMed: 27846612]

Pelus LM, Bian H, King AG, Fukuda S. Neutrophil-derived MMP-9 mediates synergistic mobilization of hematopoietic stem and progenitor cells by the combination of G-CSF and the chemokines GRObeta/CXCL2 and GRObetaT/CXCL2delta4. Blood. 2004; 103:110–119. [PubMed: 12958067]

Pulsipher MA, Chitphakdithai P, Logan BR, Shaw BE, Wingard JR, Lazarus HM, Waller EK, Seftel M, Stroncek DF, Lopez AM, et al. Acute toxicities of unrelated bone marrow versus peripheral blood stem cell donation: results of a prospective trial from the National Marrow Donor Program. Blood. 2013; 121:197–206. [PubMed: 23109243]

Pulsipher MA, Chitphakdithai P, Miller JP, Logan BR, King RJ, Rizzo JD, Leitman SF, Anderlini P, Haagenson MD, Kurian S, et al. Adverse events among 2408 unrelated donors of peripheral blood stem cells: results of a prospective trial from the National Marrow Donor Program. Blood. 2009; 113:3604–3611. [PubMed: 19190248]

Roberts AW, Foote S, Alexander WS, Scott C, Robb L, Metcalf D. Genetic influences determining progenitor cell mobilization and leukocytosis induced by granulocyte colony-stimulating factor. Blood. 1997; 89:2736–2744. [PubMed: 9108391]

Schroeder MA, Rettig MP, Lopez S, Christ S, Fiala M, Eades W, Mir FA, Shao J, McFarland K, Trinkaus K, et al. Mobilization of allogeneic peripheral blood stem cell donors with intravenous plerixafor mobilizes a unique graft. Blood. 2017; 129:2680–2692. [PubMed: 28292947]

Shaughnessy P, Chao N, Shapiro J, Walters K, McCarty J, Abhyankar S, Shayani S, Helmons P, Leather H, Pazzalia A, et al. Pharmacoeconomics of hematopoietic stem cell mobilization: an overview of current evidence and gaps in the literature. Biol Blood Marrow Transplant. 2013; 19:1301–1309. [PubMed: 23685251]

Suchankova P, Pettersson R, Nordenstrom K, Holm G, Ekman A. Personality traits and the R668Q polymorphism located in the MMP-9 gene. Behav Brain Res. 2012; 228:232–235. [PubMed: 22142952]

Switzer GE, Bruce JG, Myaskovsky L, DiMartini A, Shellmer D, Confer DL, Abress LK, King RJ, Harnaha AG, Ohngemach S, et al. Race and ethnicity in decisions about unrelated hematopoietic stem cell donation. Blood. 2013; 121:1469–1476. [PubMed: 23258921]

Switzer GE, Dew MA, Stukas AA, Goycoolea JM, Hegland J, Simmons RG. Factors associated with attrition from a national bone marrow registry. Bone Marrow Transplant. 1999; 24:313–319. [PubMed: 10455372]

Tanner RM, Lynch AI, Brophy VH, Eckfeldt JH, Davis BR, Ford CE, Boerwinkle E, Arnett DK. Pharmacogenetic associations of MMP9 and MMP12 variants with cardiovascular disease in patients with hypertension. PLoS One. 2011; 6:e23609. [PubMed: 21887284]

Tay J, Levesque JP, Winkler IG. Cellular players of hematopoietic stem cell mobilization in the bone marrow niche. Int J Hematol. 2017; 105:129–140. [PubMed: 27943116]

Tigue CC, McKoy JM, Evens AM, Trifilio SM, Tallman MS, Bennett CL. Granulocyte-colony stimulating factor administration to healthy individuals and persons with chronic neutropenia or cancer: an overview of safety considerations from the Research on Adverse Drug Events and Reports project. Bone Marrow Transplant. 2007; 40:185–192. [PubMed: 17563736]

Van den Steen PE, Van Aelst I, Hvidberg V, Piccard H, Fiten P, Jacobsen C, Moestrup SK, Fry S, Royle L, Wormald MR, et al. The hemopexin and O-glycosylated domains tune gelatinase B/MMP-9 bioavailability via inhibition and binding to cargo receptors. J Biol Chem. 2006; 281:18626–18637. [PubMed: 16672230]

Vasu S, Leitman SF, Tisdale JF, Hsieh MM, Childs RW, Barrett AJ, Fowler DH, Bishop MR, Kang EM, Malech HL, et al. Donor demographic and laboratory predictors of allogeneic peripheral blood stem cell mobilization in an ethnically diverse population. Blood. 2008; 112:2092–2100. [PubMed: 18523146]

Vu TH, Shipley JM, Bergers G, Berger JE, Helms JA, Hanahan D, Shapiro SD, Senior RM, Werb Z. MMP-9/gelatinase B is a key regulator of growth plate angiogenesis and apoptosis of hypertrophic chondrocytes. Cell. 1998; 93:411–422. [PubMed: 9590175]

Watters JW, Kloss EF, Link DC, Graubert TA, McLeod HL. A mouse-based strategy for cyclophosphamide pharmacogenomic discovery. J Appl Physiol (1985). 2003; 95:1352–1360. [PubMed: 12970373]

Waugh DJ, Wilson C. The interleukin-8 pathway in cancer. Clin Cancer Res. 2008; 14:6735–6741. [PubMed: 18980965]

Williams DA, Tao W, Yang F, Kim C, Gu Y, Mansfield P, Levine JE, Petryniak B, Derrow CW, Harris C, et al. Dominant negative mutation of the hematopoietic-specific Rho GTPase, Rac2, is associated with a human phagocyte immunodeficiency. Blood. 2000; 96:1646–1654. [PubMed: 10961859]

HIGHLIGHTS

- GROβ is well tolerated and induces mobilization in first in human study.
- Combination treatment with GROβ+AMD3100 results in rapid stem cell mobilization.
- Mouse strain nucleotide polymorphisms in MMP-9 alter biologic activity.
- Rapid mobilization releases a highly engraftable hematopoietic stem cell.

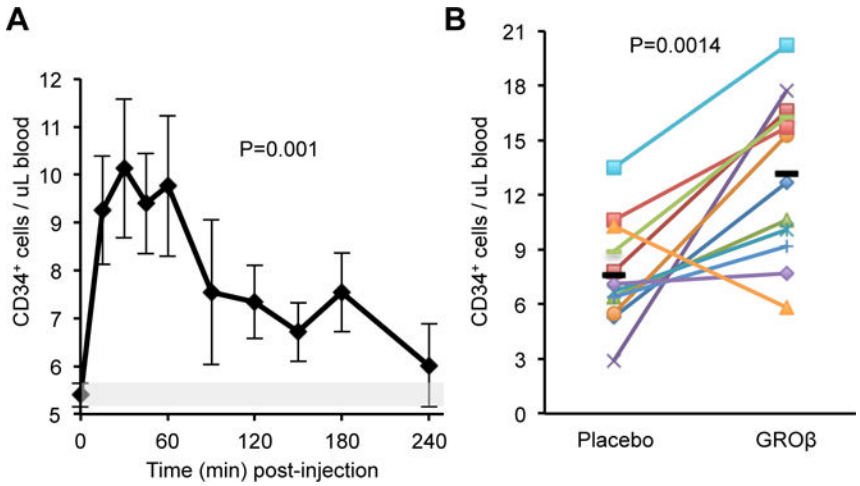

Figure 1. Peripheral blood CD34+ cells in a single blind, placebo controlled tolerability study

(A) CD34+ cells in PB following IV infusion of GROβ (N=12 subjects). Each subject received a matched placebo administration in a prior session at least 4 weeks prior to GROβ administration (grey bar; mean±SEM). P=0.001 by ANOVA.

(B) Individual maximal CD34+ cell counts after placebo or GROβ infusion. P=0.0014 by Students t-test.

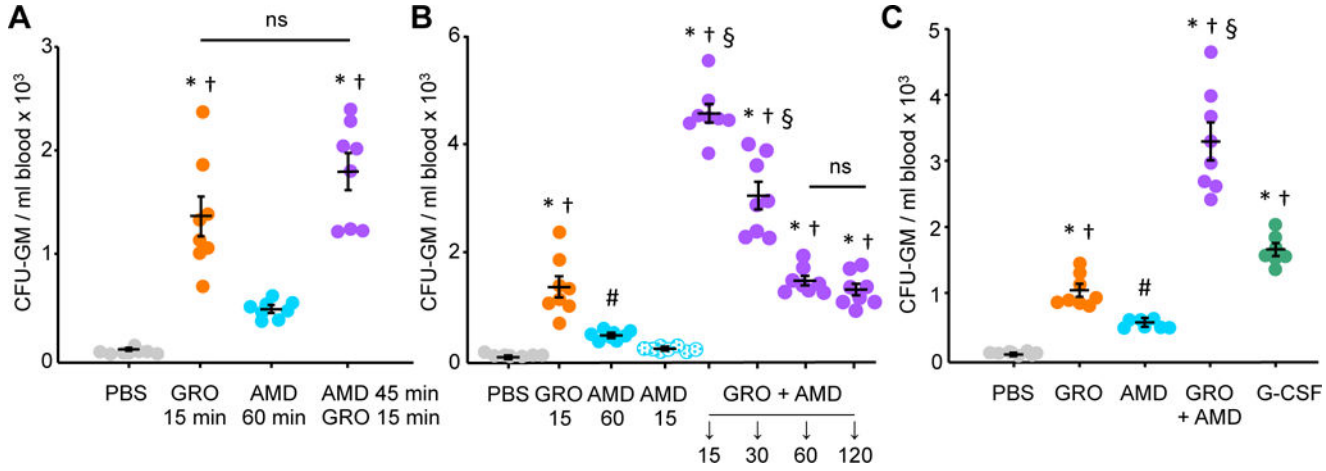

Figure 2. Timing and kinetics of single and combination mobilization in mice by GROβ and AMD3100

(A) Mean±SEM CFU-GM/ml blood mobilized at: 15 min post GROβ; 60 min post AMD3100; or 60 min post injection of AMD3100, with GROβ injected 15 min before blood harvest (45 min post AMD3100). * P<0.001 compared to control; † P<0.001 compared to AMD3100; ns = not significant, ANOVA.

(B) Mean ± SEM CFU-GM/ml blood at 15 min post GROβ; 15 and 60 min post AMD3100; and at 15, 30, 60 and 120 min post administration of GROβ+AMD3100. # P<0.05 compared to control; * P<0.001 compared to control; † P<0.001 compared to AMD3100; § P<0.001 compared to GROβ; ns = not significant, ANOVA.

(C) Mean ± SEM CFU-GM/ml blood at 15 min post GROβ, 60 min post AMD3100; and 15 min post GROβ+AMD3100, compared to mice treated with G-CSF *bid*, for 4 days. # P<0.05 compared to control; * P<0.001 compared to control; † P<0.001 compared to AMD3100; § P<0.001 compared to GROβ; ns = not significant vs. GROβ or G-CSF, ANOVA.

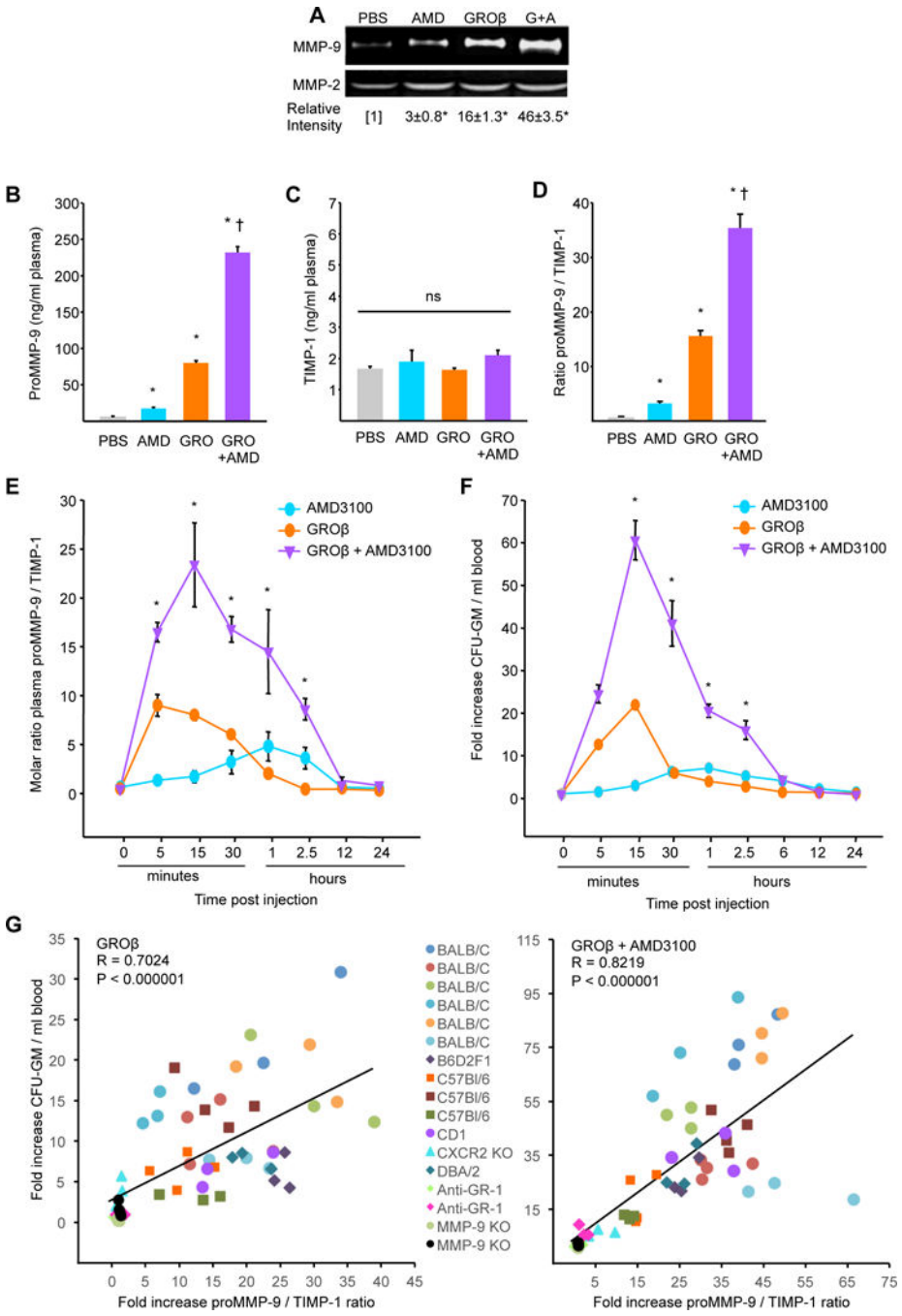

Figure 3. Combination treatment with GROβ+AMD3100 increases MMP-9 release

(A) Representative zymogram and combined relative intensities of gelatinolytic activity in plasma from Balb/c mice collected at 60 min post AMD3100; 15 min post GROβ; and 15 min post GROβ+AMD3100. Mean ± SEM from n = 8–12 mice from 2–3 experiments. * P<0.001 compared to control; ANOVA.

(B) MMP-9 and (C) TIMP-1 ELISA of mouse plasma collected at 60 min post AMD3100; 15 min post GROβ; and 15 min post combination. (D) The molar ratio of proMMP-9/ TIMP-1. Data are expressed as Mean±SEM of 4–6 Balb/c mice/group, in 1–2 experiments. *

P<0.001 vs. control or AMD3100; † P<0.001 vs. GROβ or AMD3100; ns = not significant; ANOVA.

(E) Molar ratio of proMMP-9/TIMP-1 and (F) CFU-GM in blood assessed at various time points after administration of AMD3100 and GROβ alone or in combination. Mean±SEM from n=4 Balb/c mice/group/time point. * P<0.01 vs. GROβ or AMD3100; ANOVA.

(G) Spearman's rank correlation between CFU-GM mobilized to blood and proMMP-9/TIMP-1 molar ratio after (left) GROβ or (right) GROβ+AMD3100 treatment. Each symbol represents a single mouse.

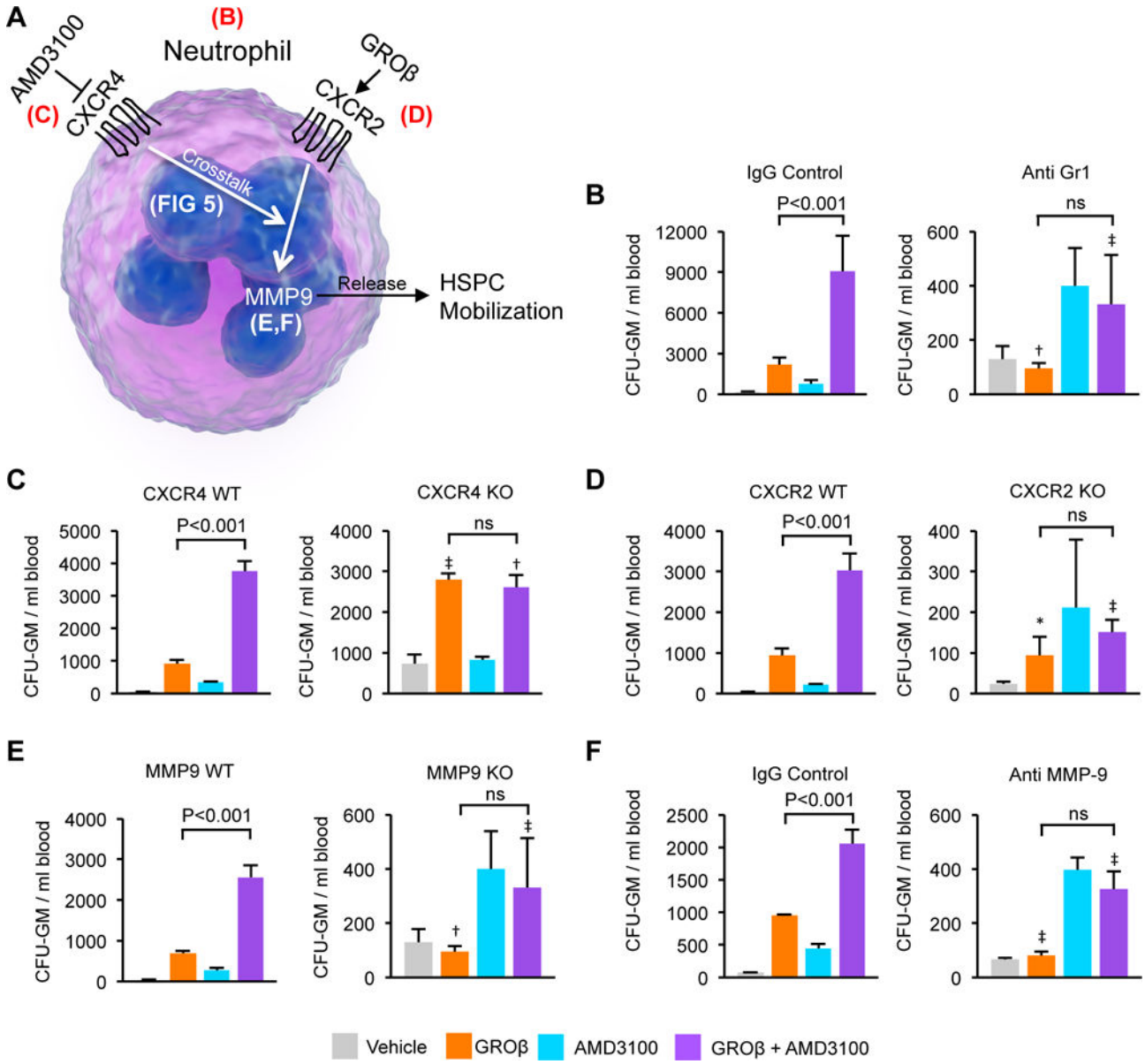

Figure 4. Crosstalk between CXCR4 and CXCR2 receptors on neutrophils enables MMP-9 release and hematopoietic mobilization

(A) Potential interaction of CXCR4 and CXCR2 signaling in neutrophils leading to MMP-9 release and hematopoietic mobilization.

(B–F) Mice were treated with GROβ, AMD3100 or combined administration as indicated. Blood was collected at 15 min post injection and CFU-GM determined.

(B) Control IgG vs. anti-GR1 antibody treatment. Mean±SEM from n=6 mice/group/2expts.

(C) Wild-type and conditional CXCR4 knockout mice. Mean±SEM from n=8 mice/group/2expts.

(D) CXCR2 wild-type and knockout mice. Mean±SEM from n=8 mice/group/2expts.

(E) MMP-9 wild-type and knockout mice. Mean±SEM from n=8 mice/group/2expts.

(F) Control IgG or anti-MMP-9 antibody to block MMP-9 activity. Data are Mean±SEM from n=4 mice/group.

In each graph, * P< 0.05, † P<0.01, ‡ P<0.001 for GROβ or GROβ+AMD3100 compared to the same groups in control or wild-type mice; ANOVA.

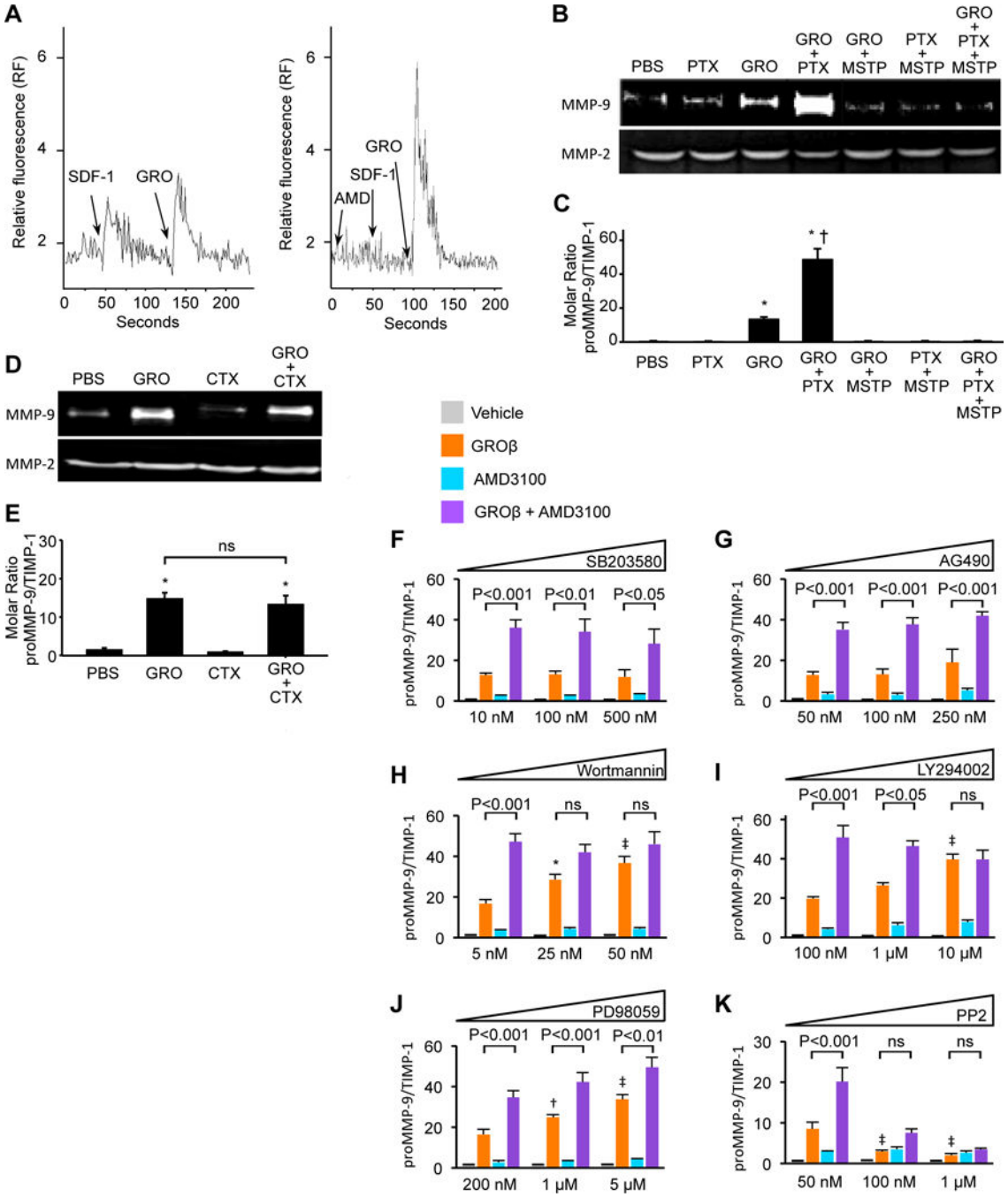

Figure 5. CXCR4 and CXCR2 signaling in human neutrophils

(A) Calcium mobilization in human neutrophils stimulated with SDF-1, GROβ (left), or AMD3100 prior to stimulation by SDF-1 and GROβ (right). One of 6 expts. using 4 different donors.

(B) Gelatinolytic activity in supernates of human peripheral blood neutrophils stimulated with PTX and/or Mastoparan prior to addition of mobilizing agents. Results are representative of 3 independent expts. using 3 different donors.

(C) Pro-MMP-9 and TIMP-1 in supernates described in (B) were determined by ELISA and molar ratio of MMP-9/TIMP-1 calculated. Mean±SEM of ELISA measurements of triplicate samples from each of 3 donors. * P<0.001 vs. PBS; † P<0.001 vs. GROβ, ANOVA.
(D) Gelatinolytic activity in supernates from neutrophils stimulated with GROβ, CTX or incubated with CTX for 15 min prior to stimulation with GROβ. Results are representative of 3 independent experiments using 3 different donors.
(E) Pro-MMP-9 and TIMP-1 in supernates described in (D) were determined by ELISA. Mean±SEM of triplicate samples from each of 3 donors. * P<0.001 vs. PBS; † P<0.001 vs. GROβ; ANOVA.
(F–K) Human PB neutrophils were incubated with the indicated intracellular signaling inhibitors for 15 min followed by stimulation with vehicle, GROβ or AMD3100 alone or in combination for 30 min. Cell free supernates were collected and MMP-9 and TIMP-1 determined by ELISA. Data represent Mean±SEM of quadruplicate cultures for each group. Each experiment was performed using freshly isolated neutrophils from a single donor, with 3 independent donors.
* P< 0.05, † P<0.01, ‡ P<0.001 vs. control. In each graph, GROβ+AMD3100 was compared to GROβ alone at each concentration of inhibitor and P values shown over brackets; ANOVA.

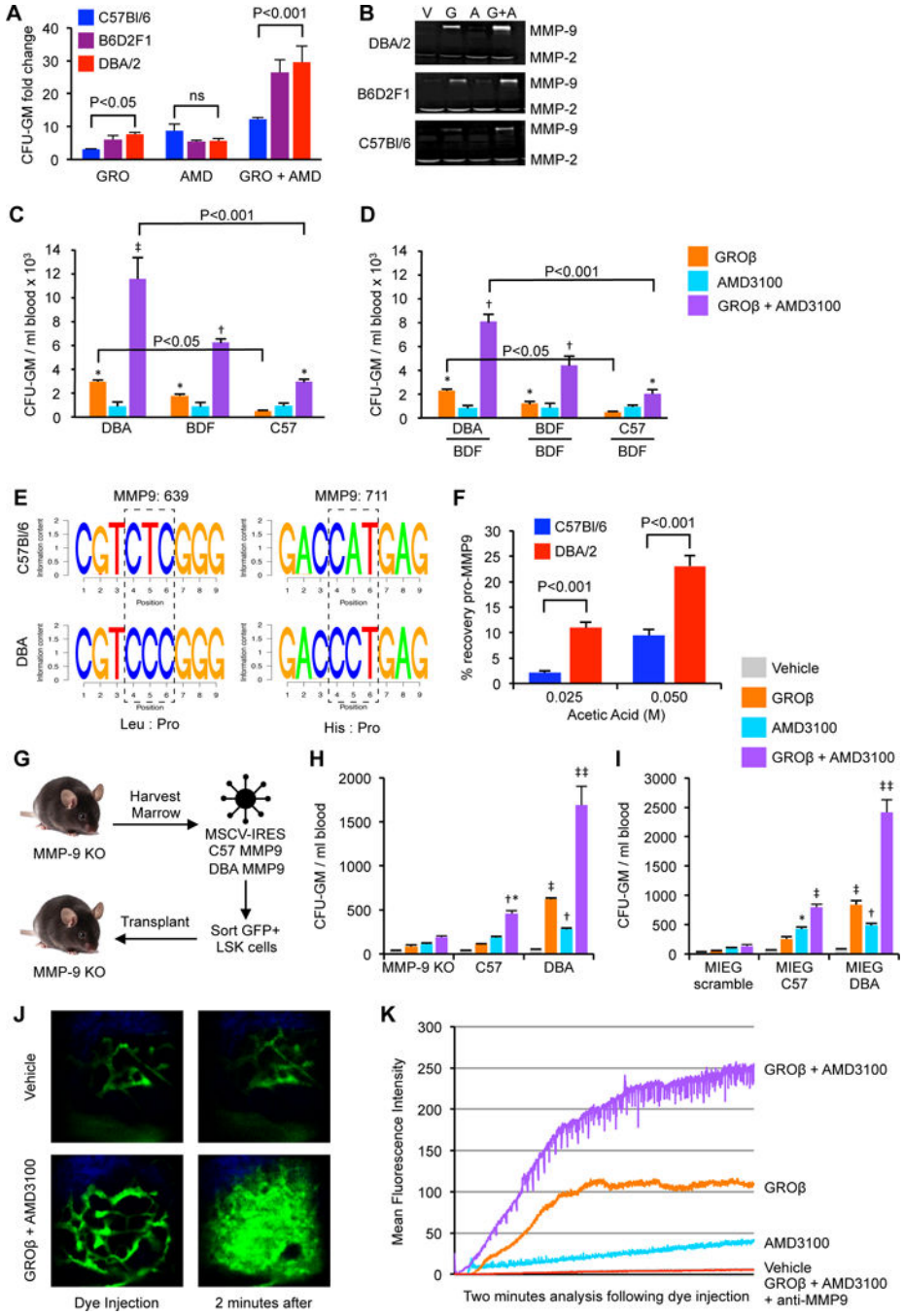

Figure 6. Strain differences in MMP-9 activity alter mobilization response

(A) Fold change in CFU-GM/ml blood at 15 min post GROβ; 60 min post AMD3100; and 15 min post GROβ+AMD3100, compared to PBS, in C57Bl/6, BDF1 and DBA/2 mice. Mean±SEM of N=4 mice/group; ANOVA.

(B) Representative zymogram of gelatinolytic activity in plasma isolated from mice collected at 15 min post vehicle (V) or GROβ (G); 60 min post AMD3100 (A) and 15 min post GROβ+AMD3100.

(C) CFU-GM/ml blood mobilized over control. Mean ± SEM of N=4 mice/group. * P<0.05, † P<0.01; ANOVA.

(D) CFU-GM/ml blood in BDF1 chimeric mice transplanted with C57Bl/6, BDF1 or DBA/2 bone marrow and treated with GROβ or AMD3100 alone and in combination at 2 months post-transplant. Mean±SEM of N=4 mice/group. * P<0.05, † P<0.01; ANOVA.

(E) Nucleotide sequence and amino acid differences in the hemoxpexin domain of the MMP-9 gene from C57Bl/6 and DBA/2 mice.

(F) Recovery of C57Bl/6 or DBA/2 MMP-9 from TIMP-1 sepharose beads after elution with acetic acid. MMP-9 was measured by ELISA. Mean±SEM of quadruplicate samples/group assayed in duplicate from one of three identical experiments. Statistical analysis by Student's T-test.

(G) Study design for transplant and transduction study in panels (H) and (I).

(H) CFU-GM/ml blood mobilized over control in MMP-9 knockout mice and wild-type C57Bl/6 and DBA/2 mice. Mean±SEM of N=4 mice/group. * P<0.05, † P<0.01, ‡ P<0.001 compared to PBS or GROβ; ANOVA.

(I) CFU-GM/ml blood mobilized over control in MMP-9 knockout mice transplanted with 2000 LSK cells transduced with DBA or C57 MMP-9 transgenes or a scrambled sequence. Mean±SEM of N=5 mice/group. * P<0.05, † P<0.01, ‡ P<0.001 compared to PBS or GROβ; ANOVA.

(J) Representative intra-vital snapshots of mouse calvaria vasculature immediately following injection of rhodamine dextran (left panels) and then 2 min later (right panels) in mice previously treated with vehicle control (top panels) or GROβ+AMD3100 (bottom panels) 5 min prior to rhodamine dextran administration (see supplemental videos 1 and 2).

(K) Representative intensity of rhodamine dextran signal outside of calvaria bone marrow vessels in mice treated with GROβ, AMD3100, GROβ+AMD3100, or mice treated with anti-MMP-9 antibody prior to administration of GROβ+AMD3100. Representative data from 2–5 mice/treatment group.

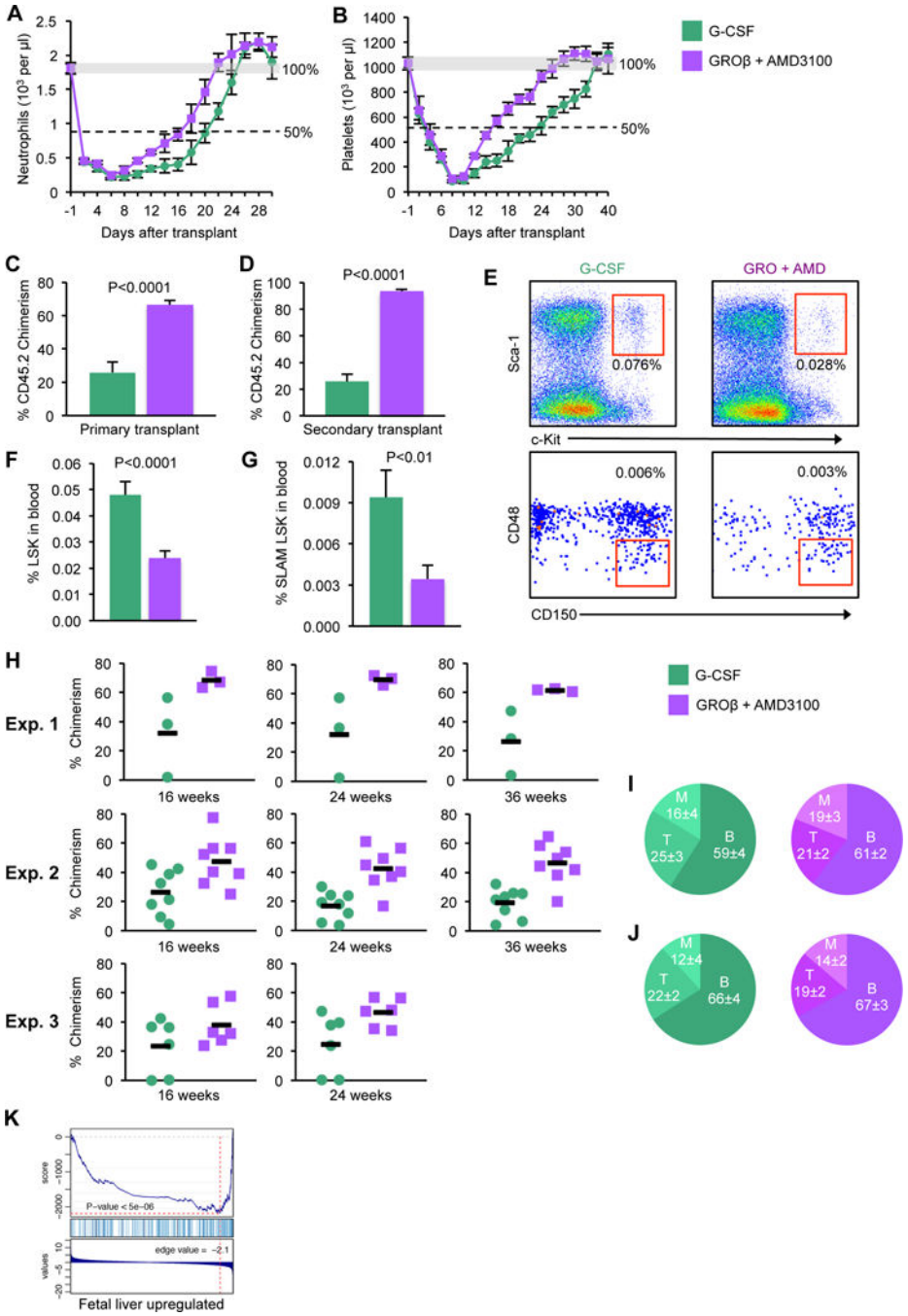

Figure 7. GROβ+AMD3100 mobilizes a hematopoietic graft with enhanced engrafting capacity

(A) Neutrophil and (B) platelet recovery in mice transplanted with PBMC from mice mobilized by G-CSF or GROβ+AMD3100. Mean±SEM of N=5 mice/group/time point, n=10 mice total/group.

(C) PB chimerism at 24 weeks post-transplantation in BoyJ mice transplanted competitively with G-CSF or GROβ+AMD3100 mobilized PBMC from C57Bl/6 mice with congenic Boy/J whole bone marrow competitors. Mean±SEM of N=11 mice/group/2expts. Statistical analysis by Student's T-test.

(D) Secondary transplantation chimerism at 24 weeks in BoyJ mice transplanted with whole bone marrow from primary recipients described in (C) taken at 24 weeks post primary transplant. Mean±SEM of N=4 primary recipient mice/group each transplanted into duplicate secondary recipients (N=8 recipients/group), with each secondary recipient assayed individually. Statistical analysis by Student's T-test.
(E) Representative LSK and SLAM-LSK frequency analysis of lineage negative PBMC from mice mobilized by G-CSF or GROβ+AMD3100.
(F) Percentage of LSK and (G) SLAM-LSK cells in peripheral blood of mobilized mice. Mean±SEM of N=13 mice from 3 independent experiments, each mouse assayed individually. Statistical analysis by Student's T-test.
(H) PB chimerism at 16, 24 or 36 weeks in BoyJ mice transplanted with 195 (Exp 1), 50 (Exp 2) or 100 (Exp 3) FACS sorted SLAM-LSK cells from PB of C57Bl/6 mice mobilized by G-CSF or GROβ+AMD3100. PB SLAM-LSK cells from GROβ+AMD3100 treated donors resulted in a 2-fold increase in competitiveness ($P<0.0004$).
(I) Tri-lineage reconstitution in mice from (H) Exp 2; N=8 and (J) in mice from Exp 3; N=6 mice. Mean±SEM, each assayed individually.
(K) SLAM LSK cells were sorted from GROβ+AMD3100 or G-CSF treated mice as performed in panel (H), and total RNA was isolated. GSEA was conducted based on the log2 fold expression ratio between GROβ+AMD3100 and G-CSF stem cells. Gene sets were taken based on data from (Ivanova et al., 2002) selecting 300 most up-regulated based on comparison of FLSca+ and BMR^{holow} samples. Statistical significance was determined based on one million randomizations.